Contrib Mineral Petrol (1992) 109:275–294

Contributions to Mineralogy and Petrology

Mildly peraluminous high-silica granites in a continental rift: the Drammen and Finnemarka batholiths, Oslo Rift, Norway

Reidar G. Trønnes and Alan D. Brandon

Department of Geology, University of Alberta, Edmonton, Canada T6G 2E3

Received April 1, 1991/Accepted July 11, 1991

Abstract. The peraluminous Drammen batholith (650 km^2) is the largest granite complex within the mainly alkaline province of the Permo-Carboniferous Oslo Rift, and peraluminous to metaluminous granites are also present in the southern part of the otherwise alkaline Finnemarka complex (125 km^2). The emplacement of the Drammen granite, and probably most of the other biotite granite complexes, predate the alkaline syenites and granites. The eight separate petrographic types of the Drammen batholith range in SiO_2 from 70 to 79 wt. % and have experienced variable amounts of fractionation of feldspars, biotite, zircon, apatite, titanite and Fe-Ti-oxides. The initial Sr, Nd and Pb isotopic ratios and a decoupling between the variations in the SiO_2 content and the aluminum saturation index [$ASI = Al_2O_3/(CaO + Na_2O + K_2O)$] show that the various intrusive phases are not strictly comagmatic. The ε_{Nd} values of the southern part of Finnemarka (+ 3.5 to + 4) and the northern part of the Drammen granite (+ 1 to + 1.5) are high and indicate insignificant (for Finnemarka) to minor Precambrian crustal or enriched mantle contributions. The very low ε_{Sr} values of all of these samples (− 1 to − 12, outside the main Oslo Rift magmatic array), point to a time integrated Rb-depleted crustal contaminant or an EM1 mantle component. The earliest extruded alkali basalts along the southwestern margin of the Oslo Rift are the only other samples within this low ε_{Sr} area, but their isotopic signature may also be linked to a mantle enrichment event (involving an EM1 component), e.g. associated with the Fen carbonatite magmatism 540 Ma ago. For a given $^{206}Pb/^{204}Pb$, the $^{208}Pb/^{204}Pb$ ratios of the Drammen and Finnemarka batholiths are distinctly lower than those of the Skien alkaline volcanics and all other magmatic Oslo Rift rocks. This may indicate that the lithosphere of the central part of the rift had a time integrated Th-depletion. The samples from the southern part of the Drammen batholith, characterized by the presence of abundant miarolitic cavities, have ε_{Nd} near 0 (− 0.7 to + 0.4) but strongly elevated ε_{Sr} of + 35 to + 67. The combined Pb isotopic ratios of all the samples analyzed indicate that the Precambrian crustal anatectic contribution is in the form of time integrated Th- and U-depleted lower crust, and the high ε_{Sr} of the sourthern part of the Drammen granite results from shallow level wallrock assimilation or magma-fluid interactions. The remarkably low contribution of old crustal components to the Finnemarka and the northernmost Drammen batholiths may result from extensive late Precambrian intracustal differentiation in southwestern Scandinavia, leading to widespread upper crustal granites (~ 900 Ma) and a correspondingly dense and refractory lower crust, in particular in a zone intersecting the central part of the rift. Liquidus phase relations and mass-balance constraints permit derivation of the granites from mildly alkaline to tholeiitic melts by extensive crystal fractionation of clinopyroxene- and amphibole-rich assemblages. It is equally possible to form the granitic magmas by partial melting of Permian gabbros of similar composition. Either scenario is consistent with the isotopic constraints and with the presence of dense cumulates and/or residues in the lower crust. The lack of igneous rocks of intermediate composition associated with the Drammen and Finnemarka batholiths point to an efficient upper crustal density filtering. Considerable amounts of heat would be accumulated in this region if differentiated, intermediate melts could not escape to shallower levels. Successive magma injections would therefore easily result in partial melting of already solidified mafic to intermediate melts and cumulates, and it is suggested that the peraluminous granites formed mainly by water-undersaturated anatexis of mafic material.

Offprint request to: R. G. Trønnes

Introduction

The Permian magmatic activity in the Oslo Rift resulted in a great variety of volcanic and plutonic rock types, mainly of alkaline affinity. The plutonic rocks occupying the presently exposed graben surface are concentrated in three main complexes, geographically separated by outcrops of Permian lavas and Cambro-Silurian sedimentary

rocks (Fig. 1). The northern Nordmarka-Hurdalen batholith is dominated by alkaline rocks of syenitic and granitic composition, although several separate intrusions of biotite granite are known from this area. Two largely monzonitic batholiths (the Larvik and Skrim massifs) occupy most of the southern rift segment, whereas biotite granites of the Drammen and Finnemarka batholiths dominate the central rift segment (Fig. 1). These batholiths cover areas of 650 and 125 km^2 respectively, and the Drammen batholith is the largest granitic complex in the rift.

The magmas of the basaltic and latitic (rhomb porphyry) lavas and the large monzonitic (larvikitic) intrusions evolved mainly by differentiation of weakly alkaline and tholeiitic basaltic magmas near the mantle-crust boundary (Neumann 1980; Neumann et al. 1985). An elongate gravity anomaly along the axis of the Oslo Rift has been associated with dense cumulates and residues from partial melting in the lower crust (Ramberg 1976; Wessel and Husebye 1987; Olsen et al. 1987; Neumann et al. 1986 and in preparation). Based on combined Sr, Nd and Pb isotope systematics and trace element chemistry, Neumann et al. (1988a) and Rasmussen et al. (1988) concluded that the anatectic crustal contribution was insignificant for some of the basalts and for most of the larvikites, but that the syenitic and granitic magmas received up to 40–50% anatectic contributions. Samples from the large biotite granite complexes in the central rift segment were not included in these studies, and chemical and isotopic variations within large intrusive bodies were not investigated.

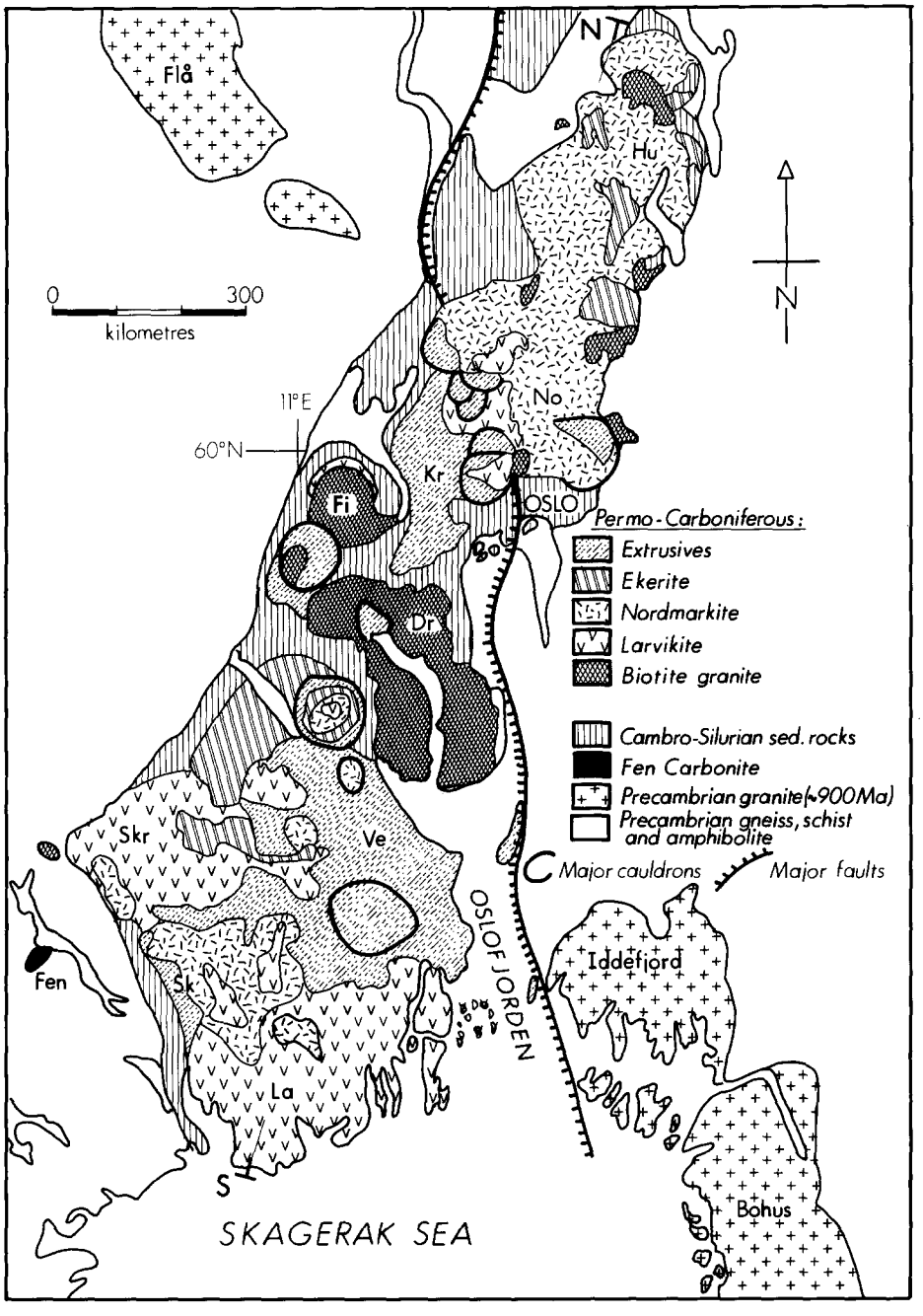

Fig. 1. Simplified geologic map of the Oslo Rift based on Sigmond et al. (1984). *Letter symbols* indicate the main lava areas (*Sk*, Skien: *Ve*, Vestfold; *Kr*, Krokskogen) and the main batholiths (*La*, Larvik; *Skr*, Skrim; *Dr*, Drammen, *Fi*, Finnemarka; *No*, Nordmarka; *Hu*, Hurdal). The letters *S* and *N* indicate the position of the simplified crustal section of Fig. 10

The peralkaline granites (ekerites with alkali pyroxenes and amphiboles) occur mostly in composite batholiths involving monzonitic and syenitic rocks, and commonly show gradual transitions into these rock types, especially in the northern rift segment. Gaut (1981) suggested a two-fold division of the biotite granites. He classified relatively early intrusions without transitions to other rock types as BG1 and late intrusions intimately associated with syenitic rocks as BG2. The mildly peraluminous Drammen granite, spatially isolated from other intrusive rocks, is the most prominent example of a BG1. Recent mapping by Stenstrop (1989), however, has shown that the most widespread rock type within the Finnemarka batholith is metaluminous to peralkaline BG2 and that peraluminous to metaluminous BG1 is confined to the southern part of the batholith. The northern Finnemarka BG2 is rimmed by intermediate intrusives, and Stenstrop (1989) suggested that the granitic rocks are derived from mafic and intermediate magmas by fractional crystallization.

The members of the BG1-category, including the Drammen batholith, are mostly older than the alkaline syenites and granites (ca. 280 Ma versus 270-240 Ma, respectively; Jacobsen and Raade 1975; Sundvoll 1978; Gaut 1981; Rasmussen et al. 1988; Sundvoll et al. 1990). It is therefore possible that these biotite granites are largely unrelated petrogenetically to the main Oslo Rift magmatic series, and several authors including Barth (1954, 1962), Killeen and Heier (1975), Ramberg (1976) and Neumann et al. (1977), suggested that they were formed by crustal anatexis. $^{87}Sr/^{86}Sr$ initial ratios, however, indicate that the source regions for the BG2 had relatively low time integrated Rb/Sr-ratios, almost indistinguishable from the other intrusives (Sundvoll 1978). Very few Sm-Nd isotopic data on the biotite granites are available, but Jacobsen and Wasserburg (1978) concluded that none of the felsic rocks, including the biotite granites, could have formed by crustal melting. The apparent contradiction between mildly peraluminous major element chemistry and isotopic mantle signatures of these voluminous intraplate granites is one of the most enigmatic features of the Oslo Rift magmatic province.

The present study of field relations, petrography and petrochemistry of the ten major intrusive phases within the Drammen granite complex, combined with Sr-Nd-Pb isotope and trace element chemistry of selected samples from the Drammen and Finnemarka (sourthern part) batholiths constrain the processes leading to peraluminous granites in a continental rift setting. In order to reconcile weakly depleted and possibly enriched mantle isotopic signatures similar to those of the Skien alkali basaltic province with the suggested early age and peraluminous chemistry of these biotite granites, granitic magma generation by fractional crystallization from mafic magmas is considered. Zen (1986) showed that differentiation of a subaluminous magma by fractional crystallization of phases with low aluminum saturation index [ASI $= Al_2O_3/(CaO + Na_2O + K_2O)$] such as clinopyroxene and amphibole can produce peraluminous granitic melts.

An alternative scenario invoking anatexis of gabbroic to clinopyroxenitic portions of the lower crust (e.g. Heltz 1976; Ellis and Thompson 1986; Beard and Lofgren 1989, 1991), possibly followed by fractionation of low-ASI pyroxenes and amphiboles, is also explored. The isotope signatures of the granites dictate that such a potential lower crustal mafic source would have formed by magmatic accretion from mantle derived melts immediately prior to or during the Permo-Carboniferous magmatic episode.

The further magmatic evolution leading to the peraluminous granites was accompanied by variable contamination by Precambrian lower crust, and the southern part of the Drammen batholith acquired high $^{87}Sr/^{86}Sr$ ratios via magma-fluid interactions or upper crustal contamination.

Intrusive phases and field relations

Petrography of the Drammen batholith

The spatial distribution of the main petrographic varieties are shown in Fig. 2. In addition to these rock types numerous aplite and pegmatite dikes, veins and irregular segregations are found throughout the area but are concentrated in the central part of the batholith. Post magmatic explosion breccias transecting the granites are observed close to the southern margin of the Drammen Caldera in the coarse-grained granite type and 4 km to the southwest in the rapakivi granite (Fig. 2).

Perthitic alkali feldspar, recording various stages of albite exsolution, is the dominant mineral in all of the granites, and small amounts of early crystallized plagioclase (oligoclase, AN_{20}) grains are present in parts of the coarse grained granite, especially in the northern area. Microline is absent from all of the granite types. Evenly distributed Fe-oxide dust throughout most of the feldspar crystals give the rocks a distinctly red colour. Partly chloritized biotite is the most abundant mafic silicate, occurring in all of the petrographic types. The biotites are most remarkable for their high F-contents (Table 1). Minor amounts of amphibole and epidote occur in the coarse-grained granite and the rapakivi granite, and small amounts of muscovite, fluorite, topaz, carbonate and pyrite are present locally, and in particular in the central part of the batholith. Fe-Ti-oxides, titanite, zircon, and apatite are widespread accessories.

The most widespread petrographic variety of the Drammen batholith is an equigranular *coarse-grained granite* (3–5 mm grain size) containing generally less than 3–5 vol. % of early crystallized oligoclase in addition to the common mineralogy of quartz (30–35 vol. %) and perthitic alkali feldspar (60–65 %). The area west of the Drammen Caldera and a 0.5–2 km wide border zone along the northeastern margin, contains a variety with up to 5–10 vol. % oligoclase. The oligoclase crystals have frequently undergone partial hydrothermal bleaching. Microscopically the late- to post-magmatic bleaching can be recognized by the precipitation of red iron oxide (hematite) along microcracks in feldspar crystals devoid of the otherwise evenly distributed Fe-oxide dust. Locally, the coarse-grained granite, and in particular the oligoclase-rich variety, contains up to 25% fine-grained interstitial groundmass.

A coarse-grained *cumulophyric granite* is confined to a 2 km wide zone along the southern margin of the batholith. Subhedral and somewhat rounded phenocrysts of perthitic feldspar, (8–15 mm) are incompletely surrounded by a interstitial medium-grained (3 mm) granitic matrix. This granite type has the highest content of the accessory minerals titanite, zircon and Fe-Ti-oxides. Gradual transitions into an equigranular *medium-* to *coarse-grained granite* occur further northwards.

South of the Drammen Caldera the coarse-grained granite is transected by a sub-circular *rapakivi granite* pluton. Zoned feldspar ovoids (5–15 mm in diameter) comprising large perthitic cores and thin albitic rims are set in a fine-grained quartz-rich groundmass (0.5–1 mm). The feldspar ovoids constitute about 50% of the rock

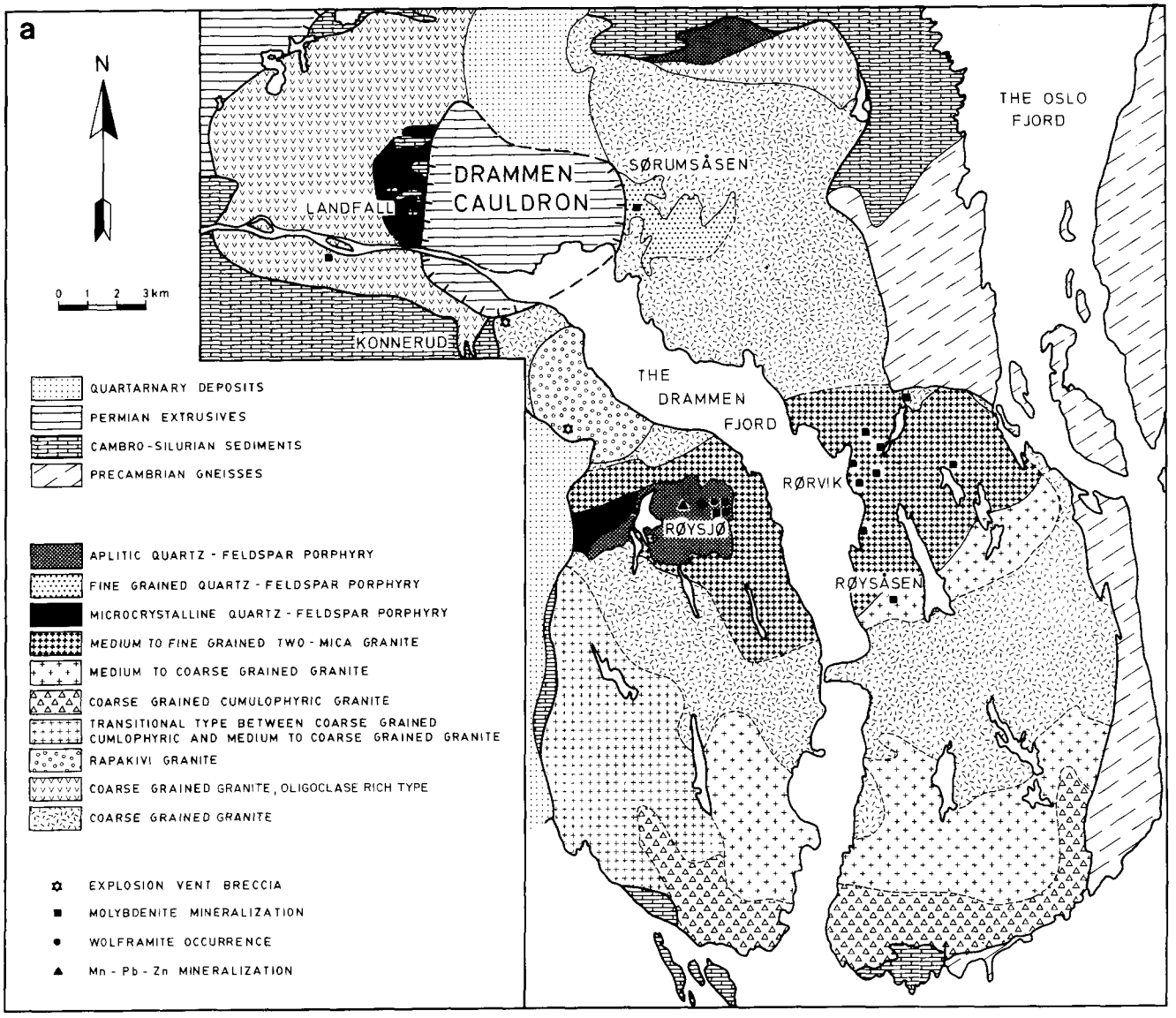

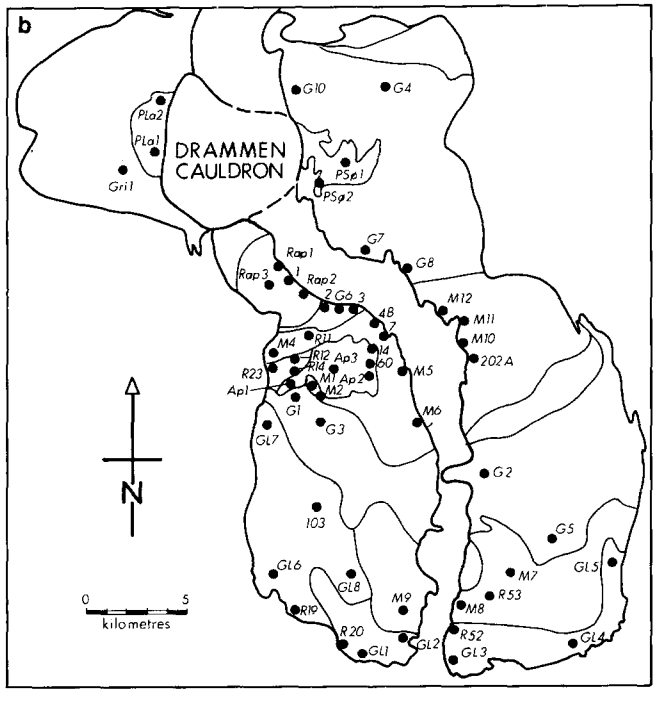

Fig. 2. a Geological map of the Drammen granite complex showing the various petrographic varieties. **b** Sample localities within the Drammen batholith. The 3 analysed samples from the sourthern part of the Finnemarka batholith have the following coordinates within UTM zone 32VNM on map sheet Lier (1814 IV, scale: 1:50000): Fi3, 667443; Fi5, 645423; Fi6, 686425

Table 1. Representative biotite compositions

Sample	*G5*	*G7*	*Gl1*	*Gl3*	*M7*	*M10*
SiO_2	39.8	40.4	40.6	40.6	39.3	38.6
Al_2O_3	11.5	11.7	10.8	11.0	14.8	15.4
TiO_2	1.87	0.32	1.41	1.44	2.18	2.11
FeO	14.0	14.8	15.6	15.9	16.4	21.6
MnO	0.79	0.83	0.38	1.31	1.25	1.95
MgO	16.5	16.3	15.9	15.7	10.6	5.28
K_2O	10.3	10.3	10.2	10.3	9.83	9.97
F	3.61	3.46	3.41	3.24	3.80	3.27
$-O \sim F$	1.52	1.46	1.44	1.36	1.60	1.38
Sum	96.85	96.65	96.86	98.13	96.56	96.80
Cations normalized to a charge of 44 (22 oxygen atoms):						
Si	5.99	6.10	6.12	6.06	5.96	6.00
Al^{IV}	2.01	1.90	1.88	1.94	2.04	2.00
Al_{VI}	0.03	0.17	0.05	0.01	0.62	0.82
Ti	0.21	0.04	0.16	0.16	0.25	0.25
Fe	1.77	1.86	1.97	1.99	2.09	2.81
Mn	0.10	0.11	0.05	0.17	0.16	0.26
Mg	3.69	3.67	3.56	3.50	2.39	1.22
K	1.97	1.98	1.96	1.97	1.91	1.98
F	1.72	1.65	1.63	4.53	1.83	1.61

Analysed by wavelength dispersive electron microprobe at Dept. of Physics, Norwegian Institute of Technology. Operating conditions were 15 kV exitation voltage and 15 nA sample current. Raster mode of analysis, correction procedures by Colby (1968) and natural mineral standards (Si, wollastonite; Al and K, orthoclase; Ti, titanite, Fe, fayalite; Mn, spessartine; Mg, spinel; F, apatite) were used. Precision and accuracy were estimated to be better than $\pm$ 5% (1σ) of the amount present for Si, Al, and F and better than $\pm$ 10% for Ti, Mn and F

volume. The primary magmatic biotite is almost completely chloritized, and epidote and amphibole are quite widespread.

The central part of the Drammen batholith is dominated by a *medium-* to *fine-grained granite*, characterized by a remarkably low content of mafic minerals. Muscovite and fluorite are more conspicious than in the other rock types. With an average grain size varying from 1 to 3 mm, the granite shows gradual transitions into the aplitic porphyry in the same area.

Three petrographic varieties of quartz-feldspar porphyries are present in the batholith. A *microcrystalline porphyry* with 3–5 mm rounded phenocrysts of quartz (30%) and perthitic alkali feldspar (70%) occurs close to the western central margin of the batholith (Røysjø area) and along the western margin of the Drammen Caldera (Landfall area), respectively. Aggregates of ilmenorutile and topaz in a limited area are most likely of post-magmatic, hydrothermal origin. Directly east of the microcrystalline porphyry in the central part of the batholith is an area of mainly quartz-phyric and leucocratic *aplite porphyry* (1–3 mm phenocrysts in a 0.5 mm groundmass). A small body of aplitic porphyry is also present along the northern border of the batholith. The *fine-grained prophyry* east of the Drammen Caldera contains 5–15 mm phenocrysts of mainly perthitic alkali feldspar and minor quartz in a 1 mm groundmass.

Field relations and intrusive sequence, Drammen batholith

The Drammen batholith intrudes Precambrian gneisses to the east and Cambro-Silurian sedimentary rocks to the north, west and south. Permian extrusives of the Glitrevann Caldera border the northwestern corner of the granite complex (Fig. 2). The emplacement of the granite batholith pre-dates the subsidence of the Drammen and Glitrevann Calderas (Gaut 1981 and Stenstrop, personal communication 1991).

Gravimetric data indicate that the batholith is a relatively thin (about 3 km thick) tabular body with one or more root-like extensions in the eastern-central area (Ramberg 1976). Alternatively the data could be interpreted as a pseudo-cylindrical body grading downwards into a mixture of stoped blocks and intrusives. The gravimetric data also indicate that the granite continues beneath the Cambro-Silurian sediments at shallow level for about 3 km southwest of the Drammen Cauldron and beneath the sedimentary rocks and gneisses for at least the same distance beyond the northeastern contact. A negative gravity anomaly along the Oslo Fjord is possibly related to a further 15–20 km subsurface extension of the batholith towards east and northeast. The calculated volume of the batholith without the latter extension is 1811 km^3 (Ramberg 1976).

Most of the granite types within the batholith seem to represent separate intrusive phases. The contact relations, however, are often unclear with gradual transitions and sharp contacts occurring at different locations along the same border between two petrographic varieties. This may be a result of the intrusion of a new magma into an already emplaced, but only partially solidified magma. Where the solidification of the early intrusion is near completion, the boundary to the new intrusion may become sharp, but where the early intrusion is still mostly liquid, a more extensive mixing and mutual assimilation may result in a transitional boundary. Partial remelting of contact portions of an early intrusive phase could also lead to transitional or ambiguous contact relations. In addition to the nature of the contacts on an outcrop scale, the topographic relations between intruded roof massifs and underlying intrusions have proven useful for the establishment of the internal intrusive sequence of the Drammen batholith.

The coarse-grained, the medium- to coarse-grained and the cumulophyric granites seem to represent the earliest intrusives of the presently exposed section of the batholith. The transitions between these varieties are mostly gradational, and they may be parts of the same intrusive event. The microcrystalline porphyries (especially in the central part of the batholith) are chemically similar to, and may be genetically related to, the coarse-grained granite. The intrusions of all of the porphyries as well as rapakivi and the medium-to fine-grained granite, however, appear to succeed the intrusion of the coarse-grained granite. In particular the fine-grained porphyry and the aplite prophyry show clear intrusive relations to this rock type.

The aplite porphyry and the medium- to fine-grained granite may be parts of the same, final intrusive phase. The porphyry is generally confined to the topographically highest areas west of the Drammen Fjord, and it may represent relatively late-stage crystallization of the magma, consistent with a viscosity increase resulting from a drop in the partial pressure of volatiles (mainly H_2O). It is also possible that the aplite porphyry intruded the medium- to fine-grained granite. Limited areas (10–100 m dimensions) of the latter type within the aplite porphyry may represent large xenolithic rafts.

Petrography and intrusive phases of the Finnemarka batholith

The internal intrusive relations within the investigated southern part of the Finnemarka complex appears to be similar to those in the Drammen batholith (Stenstrop 1989) and the central biotite granitic stock of the Glitrevann Caldera (Gaut 1981; Jensen 1985). Aphanitic to microcrystalline porphyries seem to be earlier than or approximately contemporaneous with volumetrically dominant coarse- to medium-grained granites, with final intrusive phases consisting of aplitic granites. The BG2 of the northern part of the central granitic area of the Finnemarka complex, is rimmed by quartz monzodiorite and quartz syenomonzonite, and a small gabbro intrusion immediately west of the complex may also belong to the Finnemarka magmatic series. The batholith is clearly cut by ring faults and dikes of the Glitrevann cauldron (Gaut 1981). Ramberg (1976) concluded that the intrusion is cone shaped, extending to a maximum depth of about 7.5 km, and he estimated the volume to be 336 km^3. The

Finnemarka batholith may therefore have a slightly larger average thickness (3.4 km) than the Drammen batholith (2.8 km).

Hydrothermal alteration and mineralization

Ihlen et al. (1982) described the late- to post-magmatic alteration and mineralization phenomena associated with the Drammen granite, and Olsen and Griffin (1984a, b) presented fluid inclusion data. In addition to simple exsolution of the perthitic feldspars and the hydrothermal bleaching of the early oligoclase, especially in the northern part of the batholith, the most widespread and pervasive postmagmatic alteration is albitization, mostly affecting the medium- to fine-grained granite in the central part of the batholith. The albitization seems to be closely associated with the exsolution of the perthitic alkali feldspar, and involves additional replacement of red, K-rich domains (finely dispersed Fe-oxide dust) by white (clean) albite. Extensively albitized granite areas appear bleached, and can extend over distances of less than one meter to a few hundred meters. Although bleached samples were avoided in this study, the whole rock chemistry indicates that the analysed samples of medium- to fine-grained granite and the aplite porphyry have undergone some late- and/or post-magmatic Na-enrichment. The high F-content in most of the Drammen granite samples, and especially in the medium- to fine-grained granite, indicate that the elevated Na/K-ratios may also partly be caused by the displacement of minimum melt compositions towards the albite component (e.g. Manning 1981). Mioralitic cavities and small quartz ± fluorite veins are relatively widespread within the cumuloporphyritic granite along the southern margin of the Drammen batholith.

Other hydrothermal alterations and mineralizations also occur most frequently in the central area of the batholith. These include quartz-sericite-pyrite ± topaz, sericite-chlorite, and kaolinite alterations, as well as common Mo- and rare W-mineralizations (Ihlen et al. 1982). The most important mineralizations are also indicated in Fig. 2.

Petrochemistry and isotope chemistry

Analytical procedures

The sample localities are shown in Fig. 2b. Each sample consisted of 2–4 blocks (2–3 kg each) taken within 1–3 m of each other from well-exposed outcrops, mainly road cuts. The blocks in each sample were crushed, mixed together and split to reduce the sample size before grinding. The major element oxide concentrations were determined by XRF, except for Na_2O (AAS) and FeO (wet chemical titration). The trace element analyses were performed by XRF (Rb, Sr, Ba, Y, Zr, and Nb) and INAA (lanthanides).

The XRF analyses (analyst: I. Vokes) were carried out on a Phillips PW1410 spectrometer at the University of Trondheim, Norwegian Institute of Technology using glass discs and pellets of pressed rock powder with internal Mo-standards for major and trace elements determinations, respectively. The glass discs were prepared by fusing with lithium tetraborate (Spectromelt A10). A Perkin-Elmer 503 AA spectrophotometer was used for the AAS determinations (analyst: I. Rømme).

The INAA (analyst: O. Johansen) was performed at the Institute of Energy Technology, Kjeller, using a Ge(Li) photon detector with a resolution of 2 keV at 1.33 Mev. For Ce, a low energy detector was used. The precision and accuracy estimated from the analyses of parallels and standards are ± 5% for La, Ce, Nd, Sm, Eu and Lu, ± 10% for Yb and ± 10–20% for Tb.

Sr, Nd, and Pb isotopic analyses and Rb, Sr, REE, U, Th, and Pb isotope dilution were carried out at the University of Alberta, Canada. Rb, Sr, and REE were purified using standard cation exchange procedures. Nd and Sm were separated from other REE using teflon powder saturated with HDEHP [Bis (2-ethylexyl) hydrogen phosphate] as the exchanger. Procedural blanks were < 1 ngm. for Sr and Rb and < 2 ngm. for Nd and Sm. Sr and Nd isotopic ratios were measured on an automated VG 354 five collector mass spectrometer. Replicate analyses of NBS 987 Sr metal during the course of this study were $^{87}Sr/^{86}Sr = 0.710242 \pm 6(2\sigma)$ relative to $^{86}Sr/^{88}Sr = 0.1194$ (n = 21). Replicate analyses on the La Jolla Nd standard were $^{143}Nd/^{144}Nd = 0.511856 \pm 2(2\sigma)$ relative to $^{146}Nd/^{144}Nd = 0.7219$ (n = 45). Pb isotope ratios were obtained on a VG Micromass 30 single collector mass spectrometer. Pb was purified using HBr with anion exchange resin. Whole rock procedural blanks for Pb were 300–400 pgm. 2σ analytical uncertainties, based on reproducibility on NBS 981 Pb standard by the University of Alberta isotope group are 0.05% for the ratios cited (Deb et al. 1989).

Isotope dilution on spiked aliquots of each sample was carried out for Sr, Rb, Nd, Sm, U, Th, and Pb on the VG Micromass 30 spectrometer. Precision for the measured isotopic ratios for each run was better than 1 part in 1,000 (1σ). Overall precision for the calculated abundances for all seven elements is better than or equal to ± 0.5% (2σ).

Major elements

The major element compositions of the analysed samples of the Drammen granite complex are shown in Table 2 and Fig. 3. The silica content ranges from 70 wt.% in the fine-grained porphyry to 78–79 wt.% in the aplite porphyry and the medium- to fine-grained granite. The significantly higher Na/K-ratios of the medium- to fine-grained granite and aplitic porphyry compared to the other rock types are most likely caused by late- to post-magmatic alterations (see above). The samples of the fine-grained porphyry east of the Drammen Cauldron deviate from the compositional spectrum of the other samples by their high alkalies and low CaO and P_2O_5.

The large majority of the analysed samples are peraluminous, with aluminum saturation index [ASI = molecular ratio $Al_2O_3/(Na_2O + K_2O + CaO)$ corrected for the CaO content of apatite; see Shand 1949; Zen 1986] ranging from 1.05 to 1.12 (Fig. 4). This is consistent with the appearance of small amounts of muscovite in some of the samples. The average ASI value of the four samples from the Finnemarka complex (near the southeastern margin) reported by Ihlen et al. (1982) is 1.03, similar to the 1.0 value of the only analysis of Finnemarka granite reported by Czamanske (1965). Analyses of microcrystalline and aplitic porphyries and coarse-grained granites from the southern Finnemarka area reported by Stenstrop (1989), however, cover the range from mildly peraluminous to mildly peralkaline. Other high-silica granitic rocks range in composition from peralkaline (Sierra La Primavera; Mahood 1981) to metaluminous (Bishop tuff; Hildreth 1981) to peraluminous (Sweetwater Wash pluton; Mittlefehldt and Miller 1983).

Trace elements

The trace element compositions are shown in Table 3 and Fig. 5. Analyses of some of samples for Li, F, Sn, Mo and W were reported by Ihlen et al. 1982. The common compositional spectrum of the Drammen batholith is characterized by increasing Rb and decreasing Sr, Ba, Zr, and Y with increasing degree of differentiation as gauged

Table 2. Major element analyses

Type	Sample	SiO_2	TiO_2	Al_2O_3	Fe_2O_3	FeO	MnO	MgO	CaO	Na_2O	K_2O	P_2O_5	LOI
c	2	77.0	0.26	12.6	0.59	0.27	0.04	nd	0.48	3.60	4.53	0.01	0.57
	3	75.4	0.25	13.0	1.20	0.27	0.04	0.17	0.58	3.68	4.87	0.01	0.51
	G2	75.4	0.40	13.4	0.87	0.88	0.07	0.05	0.75	3.60	4.94	0.06	0.24
	G4	76.0	0.29	13.7	0.67	0.66	0.03	0.13	0.54	3.41	5.12	0.05	0.50
	G10	75.9	0.30	13.1	0.38	0.55	0.03	0.18	0.80	3.21	5.05	0.04	0.42
	Gri1	76.3	0.33	13.8	0.59	0.72	0.03	0.32	0.81	3.03	5.14	0.05	0.04
rap	1	71.8	0.42	14.5	1.83	0.51	0.11	0.48	0.91	4.57	4.68	0.08	0.67
	Rap2	72.0	0.47	14.9	1.11	1.14	0.08	0.28	0.63	3.66	5.06	0.09	0.57
	Rap3	73.1	0.45	15.0	0.33	0.95	0.10	0.18	0.82	3.93	5.15	0.09	0.47
cum	103	73.7	0.40	13.8	1.49	0.13	0.04	nd	0.67	4.16	4.83	0.02	0.62
	R19	72.7	0.44	13.5	1.59	0.65	0.04	0.25	0.85	3.97	5.01	0.04	0.95
	R20	76.4	0.31	12.5	1.08	0.59	0.02	0.28	0.46	3.52	4.23	0.03	0.74
	R52	72.6	0.38	13.3	1.47	0.54	0.07	0.27	0.65	4.18	4.72	0.03	0.28
	Gl1	73.7	0.45	13.5	1.11	0.87	0.08	0.07	0.70	4.35	5.12	0.06	0.39
	Gl4	75.4	0.47	13.4	1.23	0.65	0.06	nd	0.52	4.02	5.07	0.06	0.51
	Gl5	76.4	0.37	12.4	0.95	0.72	0.03	nd	0.28	3.48	4.82	0.04	0.61
m-c	*R53*	74.1	0.42	12.9	1.49	0.23	0.03	0.24	0.61	4.07	4.98	0.02	0.69
	M7	73.8	0.42	12.9	1.02	0.66	0.05	0.03	0.47	3.81	5.13	0.06	0.41
	M8	74.5	0.36	13.3	0.83	0.67	0.05	0.09	0.63	4.05	5.08	0.04	0.05
m-f	4B	76.3	0.11	12.8	0.99	0.27	0.03	0.07	0.55	3.95	4.34	nd	0.46
	7	77.0	0.14	12.7	0.53	0.44	0.04	0.02	0.51	3.89	4.14	nd	0.39
	202A	77.2	0.13	12.5	0.52	0.46	0.04	0.22	0.54	3.78	4.16	nd	0.38
	R11	77.3	0.12	12.5	0.67	0.12	0.03	0.03	0.47	3.77	4.26	nd	0.70
	M1	78.5	0.20	12.5	0.30	0.35	0.02	nd	0.17	3.75	4.51	nd	0.48
	M5	78.9	0.16	12.5	0.24	0.33	0.03	nd	0.39	3.57	4.71	nd	0.45
	M6	76.9	0.09	13.2	0.56	0.16	0.01	nd	0.18	4.28	4.64	nd	0.33
apl-p	14	77.6	0.12	12.6	0.38	0.30	0.03	nd	0.29	3.95	4.22	nd	0.30
	60	78.0	0.15	12.4	0.67	0.21	0.02	0.06	0.36	3.58	4.39	nd	0.28
	Ap1	78.5	0.16	12.8	0.40	0.33	0.02	nd	0.21	3.60	4.70	0.01	0.35
	Ap2	77.6	0.12	13.2	0.38	0.29	0.01	nd	0.31	4.26	4.60	0.02	0.32
mi-p-R	*R12*	75.4	0.26	12.9	0.67	0.27	0.02	0.20	0.81	3.78	5.24	0.01	0.52
	R14	75.0	0.34	13.4	0.94	0.37	0.01	0.12	0.22	4.22	4.09	0.03	0.52
	R23	75.6	0.30	13.5	0.57	0.28	0.02	nd	0.29	3.95	4.90	0.01	0.48
mi-p-L	*PLa1*	76.0	0.29	13.1	0.27	0.67	0.04	0.06	0.85	3.29	5.19	0.03	0.96
	PLa2	77.5	0.28	12.5	0.40	0.29	0.02	nd	0.15	3.05	5.20	0.02	0.72
f-p	*PSϕ1*	70.6	0.48	15.1	1.56	0.68	0.08	nd	0.50	5.18	5.34	0.05	0.69
	PSϕ2	70.3	0.45	15.4	1.72	0.47	0.05	nd	0.19	5.19	5.33	0.05	0.56

Values in weight percent; nd, not detected. LOI, loss on ignition; rock type symbols: c, coarse-grained granite; rap, rapakivi granite; cum, cumuloporphyritic granite; m-c, medium- to fine-grained granite; m-f, medium- to coarse-grained granite; apl-p, aplitic porphyry; mi-p, microcrystalline porphyry (R and L indicate location, Rϕysjϕ and Landfall, respectively, see Fig. 2); f-p, fine grained porphyry

by increasing silica (Fig. 5). Relative to this compositional trend the fine-grained porphyry is depleted in Sr, Ba and Y, and the rapakivi granite is depleted in Y. The Nb-contents do not show any systematic enrichment or depletion with increasing differentiation. The F-contents vary from 0.02 to 0.23 wt.%, and are generally higher in the central and southern part of the Drammen batholith. Volatile degassing prior to or during the crystallization of the aplitic porphyry may be responsible for the lower F-concentrations in this rock type relative to the medium- to fine grained granite.

The Rb -SiO_2 variation is relatively smooth in the 70–77% silica range, but the medium- to fine-grained granite and aplitic porphyry (77–79% silica) have considerably higher and more variable Rb-contents. The suspected mobility of the alkalies (Figs. 3 and 5) in the hydrothermally overprinted central core of the Drammen batholith is consistent with the observed disturbance of the Rb-Sr isotopic system (see later).

Chondrite normalized REE-values for the different granite types are plotted in Fig. 6. All of the granite types are LREE-enriched, and the medium- to fine-grained

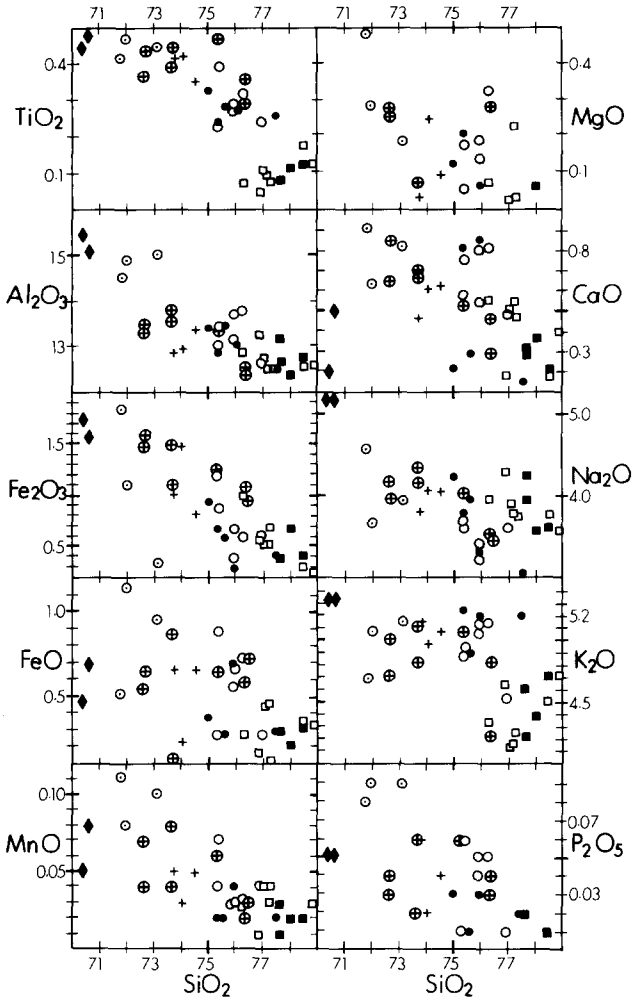

Fig. 3. Major element variation in weight percent. *Solid diamonds*: fine grained porphyry; *circles with dots*: rapakivi granite; *circles with crosses*: cumuloporphyritic granite; *crosses*: medium- to coarse-grained granite; *open circles*: coarse-grained granite; *dots*: microcrystalline porphyry; *open squares*: medium to fine-grained granite: *solid squares*: aplitic porphyry

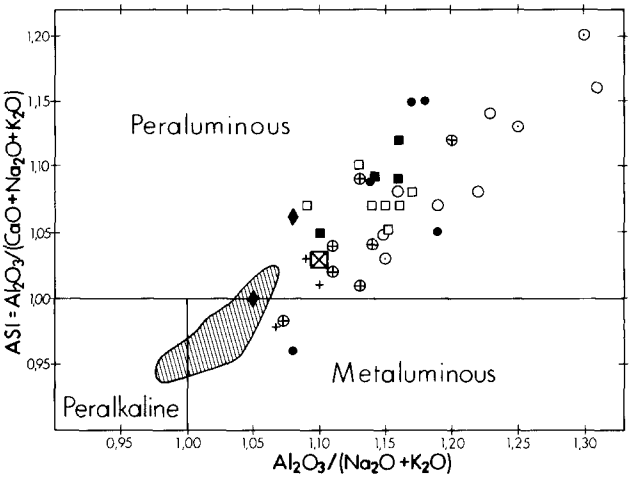

Fig. 4. Aluminum saturation index (ASI) versus inverse agpaitic index ($Al_2O_3/Na_2O + K_2O$) with boundaries according to Shand (1943). The ASI-ratio is corrected for the CaO-content of apatite (Zen 1986), assuming that all P_2O_5 is present as apatite. The *hatched area* is the compositional field of the granitic stock of the Glitrevann Caldera directly north of the Drammen granite (Fig. 1; Jensen 1985). Contrary to the Drammen batholith samples, the Glitrevann stock shows a regular compositional evolution from peraluminous (least differentiated granites) via metaluminous to peralkaline (most differentiated granites). Symbols as in Fig. 3

granite and the aplite porphyry are also HREE-enriched. The patterns are sub-parallel, and the combined REE-contents decrease from maximum values in the cumuloporphyritic granite ($La_n = 250$, $Tb_n = 43$) to minimum values in the aplite porphyry ($La_n = 100$, $Tb_n < 1$). Negative Eu-anomalies of varying degrees are found in all of the samples.

The four analyses of Finnemarka granite in Ihlen et al. (1982) and the three analyses reported here are characterized by higher and more variable contents of Li, F, and especially Nb compared to the Drammen batholith compositional spectrum.

Sr-Nd isotopic relations

The Rb-Sr and Sm-Nd isotope ratios of selected samples from the Drammen and Finnemarka granite complexes are listed in Table 4. ε_{Sr} and ε_{Nd} are calculated at 280 Ma, following Jacobsen and Wasserburg (1984) and Allegre et al. (1983). Also listed are Nd model ages (T_{DM}) calculated relative to a hypothetical depleted mantle following DePaolo (1981). ε_{Sr} values in the Drammen complex range from -10 to -1 for samples in the northern part of the complex (coarse-grained granite), to $+35$ to $+67$ for samples in the southern part of the complex (medium-grained granite and coarse cumulophyric granite). Samples from the central part of the complex show anomalous values of ε_{Sr} ranging from $+556$ to -9148, consistent with the observed mobility of the alkalies (Na, K and Rb) in the aplitic porphyry and medium- to coarse-grained granite. The microcrystalline porphyry (Fi3) from the Finnemarka complex has ε_{Sr} of -12, the most non-radiogenic Sr of the unaltered samples, whereas the coarse-grained granite (Fi5) has an anomalously low value of -98.

The ε_{Nd} values generally correlate with the ε_{Sr} values with more radiogenic Nd ratios matching nonradiogenic Sr ratios for both the Finnemarka and Drammen complexes. The ε_{Nd} values of the samples from the Finnemarka batholith ($+3.7 \pm 1$) and the northern part of the Drammen batholith ($+0.8$ to $+1.6$) are remarkably high for granitic rocks emplaced within a Precambrian continental crust. The T_{DM}(Nd) model ages are correlated with ε_{Nd} and ε_{Sr}, and vary systematically with younger, late-Proterozoic (600 Ma) values for the Finnemarka to 1220 Ma in the southern part of the Drammen batholith (Table 4).

Figure 7 displays ε_{Nd} versus ε_{sr} for Oslo Rift igneous rocks. The Finnemarka granite sample lies within the range for the mildly depleted mantle (MDM) that may have underlain the Oslo Rift during the Permian (Neumann et al. 1988a; 1990). This mantle source is defined by the rocks that are most primitive isotopically, i.e. some of the

Table 3. Trace element analyses

Type	Sample	F	Rb	Sr	Ba	Y	Zr	Nb	La	Ce	Nd	Sm	Eu	Tb	Yb	Lu
c	2	400	256	72	—	31	165	79	—	—	—	—	—	—	—	—
	3	750	294	96	—	49	141	45	—	—	—	—	—	—	—	—
	G1	400	296	64	300	55	284	56	67	115	42	8.1	0.9	1.0	7.1	0.86
	G2	1400	233	88	320	63	279	74	50	104	—	—	1.1	—	—	0.84
	G3	1400	247	76	290	60	214	59	51	108	—	—	1.1	—	—	0.83
	G4	250	233	98	400	18	121	15	44	72	23	4.1	0.5	0.4	3.7	0.37
	G5	1700	222	72	280	81	280	57	50	98	—	—	1.1	—	—	0.89
	G6	1200	297	78	190	56	140	58	41	94	—	—	0.6	—	—	0.83
	G7	250	235	106	460	25	149	33	43	65	23	4.4	0.6	0.4	3.4	0.38
	G8	1300	294	71	190	58	155	62	45	55	—	—	0.5	—	—	0.93
	G10	600	247	110	400	31	144	31	36	66	—	—	0.6	—	—	0.49
	Gri1	600	231	98	400	36	151	32	52	84	28	5.4	0.6	0.7	4.0	0.48
rap	1	650	186	168	—	31	283	64	—	—	—	—	—	—	—	—
	Rap1	200	196	158	420	26	257	70	78	113	38	6.2	0.9	0.8	4.0	0.45
	Rap2	250	200	148	420	36	300	81	—	—	—	—	—	—	—	—
	Rap3	450	196	162	420	36	311	75	—	—	—	—	—	—	—	—
cum	103	1100	205	92	—	59	417	69	—	—	—	—	—	—	—	—
	R19	950	205	82	—	85	540	51	—	—	—	—	—	—	—	—
	R20	200	227	104	—	31	192	41	—	—	—	—	—	—	—	—
	R52	1050	179	107	—	60	341	52	—	—	—	—	—	—	—	—
	Gl1	1200	212	76	340	79	406	—	97	162	67	14	1.7	1.7	7.1	0.97
	Gl2	1800	239	60	220	77	309	75	74	134	57	12	1.2	1.8	8.0	1.0
	Gl3	1400	230	97	370	78	428	97	88	161	66	14	1.6	1.6	8.5	1.1
	Gl4	950	214	68	300	120	319	70	72	142	77	19	1.7	3.0	9.9	1.2
	Gl5	400	224	62	200	39	322	89	—	—	—	—	—	—	—	—
	Gl6	1800	242	27	170	71	349	87	—	—	—	—	—	—	—	—
	Gl7	1400	252	58	220	59	289	65	—	—	—	—	—	—	—	—
	Gl8	1300	228	71	290	61	293	67	—	—	—	—	—	—	—	—
m-c	*R53*	750	217	84	—	61	313	71	—	—	—	—	—	—	—	—
	M7	1200	243	41	220	77	354	87	—	—	—	—	—	—	—	—
	M8	650	223	61	280	55	270	70	—	—	—	—	—	—	—	—
	M9	1100	217	69	290	76	299	61	—	—	—	—	—	—	—	—
m-f	4B	2250	372	49	—	61	120	73	—	—	—	—	—	—	—	—
	7	2200	408	41	—	33	117	58	—	—	—	—	—	—	—	—
	202A	2250	415	28	—	73	149	86	—	—	—	—	—	—	—	—
	R11	1450	630	24	—	42	105	115	—	—	—	—	—	—	—	—
	M1	300	287	19	60	43	147	58	32	57	17	3.1	0.3	0.4	6.4	0.82
	M2	250	273	20	60	29	119	54	—	—	—	—	—	—	—	—
	M4	2300	619	9	30	50	107	115	38	63	8	1.9	0.1	0.3	7.5	1.0
	M5	400	427	6	30	53	148	78	—	—	—	—	—	—	—	—
	M6	300	548	8	20	55	190	116	27	38	8	1.9	nd	0.2	9.5	1.6
	M10	2300	378	25	30	87	145	88	—	—	—	—	—	—	—	—
	M11	1600	393	23	50	41	104	68	30	41	12	2.1	0.2	0.2	4.3	0.7
	M12	1600	354	29	70	37	118	48	—	—	—	—	—	—	—	—
apl-p	14	550	426	26	—	18	139	74	—	—	—	—	—	—	—	—
	60	900	332	32	—	12	110	68	—	—	—	—	—	—	—	—
	Ap1	400	407	6	20	15	150	72	36	41	7	0.9	0.1	nd	1.5	0.31
	Ap2	350	291	16	15	18	98	57	32	44	7	1.5	nd	0.2	5.7	0.80
	Ap3	850	426	11	20	26	155	75	41	47	8	1.0	0.1	nd	1.9	0.25
mi-p-R	*R12*	450	309	74	—	24	166	67	—	—	—	—	—	—	—	—
	R14	450	222	93	420	52	248	54	67	117	48	9.8	1.3	1.3	7.2	0.91
	R23	700	279	83	—	44	244	65	—	—	—	—	—	—	—	—
mi-p-L	*PLa1*	450	263	89	200	39	160	42	54	80	27	5.9	0.5	0.6	4.6	0.56
	PLa2	200	265	51	190	31	147	41	—	—	—	—	—	—	—	—
f-p	*PSø1*	550	141	32	140	55	617	69	—	—	—	—	—	—	—	—
	PSø2	200	161	29	170	47	654	62	85	178	55	10	1.8	0.9	6.1	0.84
Finnem	*Fi3*	300	197	40	150	59	336	140	51	104	41	8.5	1.3	1.2	7.4	0.83
	Fi5	2500	215	33	100	53	361	169	55	103	39	7.5	1.2	0.7	9.3	0.88
	Fi6	2400	272	29	70	40	210	134	55	96	26	4.3	0.7	0.6	7.1	0.62

Values in ppm. nd, not detected. Rock type symbols as in Table 3; three samples from the southeastern part of the Finnemarka complex are included: Fi3 is a microcrystalline porphyry, Fi5 is a coarse grained and Fi6 is an aplistic porphyry

larvikites, basalts and rhomb pophyries. The samples from the northern part of the Drammen complex (Gri1, G4 and G7) lie to the left of (lower ε_{Sr} than) the main Oslo Rift magmatic array of basalts, latites (rhomb porphyries), larvikites, syenites and other granitic rocks. The main magmatic array may be plausibly interpreted as mixing lines between MDM and lower and upper crustal sources present in southeastern Norway (Neumann et al. 1988a).

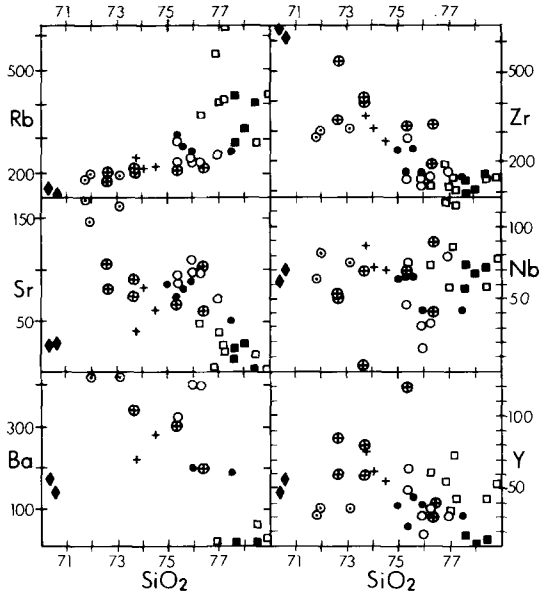

Fig. 5. Trace element variation diagrams (silica along the abscissa). Symbols as in Fig. 3

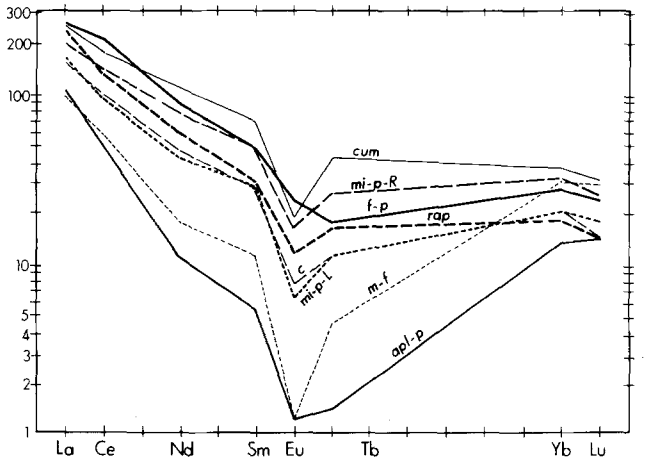

Fig. 6. Chondrite normalized (sample concentration/average chondrite concentration) lanthanide patterns for the various granite types (average values calculated from the data in Table 3). Letter codes as in Tables 2 and 3 [*c*, coarse-grained granite; *rap*, rapakivi granite: *cum*, cumuloporphyritic granite: *m-f*, medium- to fine-grained granite; *apl-p*, aplitic porphyry; *mi-p*, microcrystalline porphyry (*R* and *L* indicate location, Røysjø and Landfall, respectively; see Fig. 2); *f-p*, fine-grained porphyry]

The only other rocks from the Oslo Rift that have the Sr-Nd isotopic characteristics of the Finnemarka complex and the northern part of the Drammen batholith are the Skien lavas (alkali basalts, basanites, and nephelinites) exposed at present along the southwestern margin of the Rift (Fig. 1, Neumann et al. 1988a; Anthony et al. 1989). The samples from the southern part of the Drammen batholith (G11, G13, G14 and M9) plot within the common Oslo Rift magmatic array (Fig. 7).

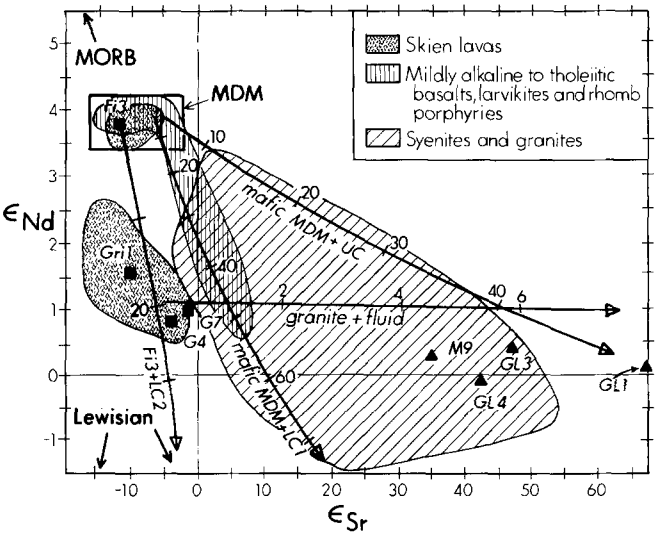

Fig. 7. Initial ε_{Sr}-ε_{Nd} relations for the Finnemarka and Drammen samples from Table 4 (*large solid squares* and *triangles* with sample designations) and other Oslo Rift magmatic rocks from Neumann et al. (1988a, Table 1) and Anthony et al. (1989, Table 2). The *box* labelled MDM encloses the mildly depleted mantle source for the Oslo rift magmas proposed by Neumann et al. (1988a). Possible *mixing lines* involving a basaltic composition with MDM isotopic signature (mafic MDM) are from Neumann et al. (1988a) and point towards the following model reservoirs: *UC*, upper crust in southeast Norway based on average values of granites, gneisses and amphibolites in southern Telemark (ε_{Sr} = 748, Sr = 119 ppm, ε_{Nd} = − 5.9, Nd = 76 ppm) and *LC*1, a model composition of the intermediate to lower crust differing from the upper crustal model only with respect to ε_{Sr} = 150. The two other *mixing lines* involve granitic melts (granite, average of Gri 1, G4 and G7); *LC*2 is a model lower crust differing from LC1 only with respect to ε_{Sr} = 0 and *fluid* is a Permian upper crustal fluid based on the upper crust model and on fluid inclusions in the Drammen granite (ε_{Sr} = 748, Sr = 120 ppm, ε_{Nd} = − 5.9, Nd = 7 ppm; see Fig 2 in Neumann et al. 1988a). The *arrow marked MORB* points towards a strongly depleted mantle source, and the *arrows marked Lewisian* point towards a range of granulite facies lower crustal compositions (Dickin 1981). The proportions (%) of the crustal components are indicated along the mixing lines

U-Th-Pb isotopic relations

U, Th, and Pb isotope ratios for selected samples are listed in Table 5. The samples from the central core of the Drammen batholith with suspected alkali element mobility ratios and disturbed Rb-Sr isotope system were excluded from this study. Initial Pb ratios at 280 Ma were calculated using ^{238}U, ^{235}U, and ^{232}Th decay constants reported in Neumann et al. (1988a) to insure a consistent correction for comparable Oslo Rift samples. Initial $^{206}Pb/^{204}Pb$ versus $^{207}Pb/^{204}Pb$ ratios for the Oslo Rift samples (Neumann et al. 1988a) plot in an array between postulated mildly depleted mantle source (MDM) and known and postulated crustal compositions in SE Norway (Fig. 8). This mixing trend appears to indicate mainly lower, rather than upper, crustal contributions. Neumann et al. (1988a) showed that this array also corresponds to a secondary isochron with an age of 290 Ma.

Fi3, the most primitive of the granite samples in terms of the ε_{Sr}–ε_{Nd} variation, falls just outside the Oslo Rift

Table 4. Rb-Sr and Sm-Nd isotopic data

Type	Sample	Sr	Rb	$^{87}Rb/^{86}Sr$	$^{87}Sr/^{86}Sr_0$	$^{87}Sr/^{86}Sr_{280}$	εSr_{280}
c	*G4*	92.0	237.3	7.480	0.733615(11)	0.70385	− 4
	G7	99.3	232.6	6.7907	0.731135(15)	0.70408	− 1
	Gri1	91.5	237.9	7.544	0.733511(29)	0.70345	− 10
apl-p	*Ap3*	6.57	388.0	182.57	1.410430(36)	0.68306	− 300
m-f	*M5*	5.93	409.3	217.4	1.609528(41)	0.74333	+ 556
	M6	2.30	525.8	874.6	3.54385(12)	0.05971	− 9148
m-c	*M9*	65.2	227.6	10.131	0.746971(17)	0.70661	+ 35
cum	*Gl1*	81.9	210.9	7.477	0.738627 (11)	0.70884	+ 67
	Gl3	91.6	224.6	7.108	0.735774(17)	0.70746	+ 47
	Gl4	67.0	209.5	9.081	0.743296(15)	0.70712	+ 42
Finnem	*Fi3*	35.8	185.8	15.072	0.763357(25)	0.70331	− 12
	Fi5[a]	23.7	212.3	26.16	0.80246(24)	0.69822	− 84
	Fi5[a]	24.8	210.6 211.7	24.733	0.794773(29)	0.69624	− 112

Type	Sample	Nd	Sm	$^{147}Sm/^{144}Nd$	$^{143}Nd/^{144}Nd_0$	$^{143}Nd/^{144}Nd_{280}$	εNd_{280}	T_{DM}
c	*G4*	23.0	3.75	0.0986	0.512503(6)	0.51232	+ 0.8	757(Ma)
	G7	22.7	3.90	0.1039	0.512524(6)	0.51233	+ 1.0	764
	Gri1	30.0	5.19	0.1047	0.512549(7)	0.51236	+ 1.6	736
apl-p	*Ap3*	5.51	0.669	0.0735	0.512373(6)	0.51224	− 0.7	763
m-f	*M5*	23.6	4.30	0.1102	0.512488(5)	0.51229	+ 0.3	856
	M6	8.91	1.59	0.1080	0.512437(6)	0.51224	− 0.7	908
m-c	*M9*	63.9	12.62	0.1195	0.512508(5)	0.51229	+ 0.3	904
cum	*Gl1*	69.0	13.45	0.1179	0.512501(5)	0.51228	+ 0.1	900
	Gl3	78.6	15.46	0.1190	0.512523(5)	0.51230	+ 0.4	877
	Gl4	79.7	19.81	0.1506	0.512542(10)	0.51227	− 0.1	1220
Finnem	*Fi3*	47.7	8.65	0.1097	0.512672(5)	0.51247	+ 3.8	602
	Fi5	52.0	9.48	0.1103	0.512664(5)	0.51246	+ 3.6	616

Rock type symbols as in Tables 2 and 3; [a],duplicate analyses; all ratios relative to $^{86}Sr/^{88}Sr = 0.1194$ and $^{146}Nd/^{144}Nd = 0.7219$; $^{87}Rb/^{86}Sr_{UR} = 0.0827$; $\lambda(^{87}Rb) = 1.42*10^{-12}yr^{-1}$; $^{87}Sr/^{86}Sr_{UR0} = 0.7045$; $^{87}Sr/^{86}Sr_{UR_{280}} = 0.70415$; $\lambda(^{147}Sm) = 6.54*10^{-12}yr^{-1}$; $^{147}Sm/^{144}Nd_{CHUR} = 0.1967$; $^{143}Nd/^{144}Nd_{CHUR_0} = 0.512638$; $^{143}Nd/^{144}Nd_{CHUR_{280}} = 0.512277$; T_{DM} after DePaolo (1981). The precision in the sixth place (2σ) for measured isotopic ratios are shown in parantheses

magmatic rock array and outside the proposed MDM field in the direction of a strongly depleted mantle (SDM) at 280 Ma (MORB source mantle). The other samples plot inside the common magmatic rock array, and partly inside the MDM field. Figure 8 shows that the initial $^{208}Pb/^{204}Pb$ for a given $^{206}Pb/^{204}Pb$ ratio is significantly lower in the Finnemarka and Drammen samples than in the Oslo Rift samples analyzed by Neumann et al. (1988a). Correspondingly low $^{208}Pb/^{204}Pb$ ratios for galena concentrates from intramagmatic and contact metasomatic mineralizations of the Drammen batholith relative to most of the other magmatic and hydrothermal systems of the Oslo Rift were observed by Bjørlykke et al. (1990). Relatively low $^{208}Pb/^{204}Pb$ ratios are also encountered in magmatic rocks and mineralizations immediately west of the Drammen batholith (syenites in the Sande Cauldron analyzed by Neumann et al. 1988a and Pb-Zn-mineralizations in the northeastern part of the main ekerite massif in the southern rift segment analyzed by Biørlykke et al. 1990), possibly indicating time-integrated Th-depletion in the lithosphere underlying the central part of the rift.

Discussion

Isotopic and chemical constraints on source materials

The negative ε_{Sr} and positive ε_{Nd} of the samples from the Finnemarka and northernmost part of the Drammen granite (the coarse-grained granite) are consistent with an origin of these granites from mantle-derived sources, with minimal contamination by pre-existing (Precambrian) crust. Two scenarios are equally plausible: (1) fractionation of mantle-derived basaltic magma; and (2) partial

Table 5. U-Th-Pb isotopic data

Type	Sample	U	Th	Pb	$^{238}U/^{204}Pb$	$^{232}Th/^{238}U$	$^{206}Pb/^{204}Pb_0$	$^{207}Pb/^{204}Pb_0$	$^{208}Pb/^{204}Pb_0$
c	*G4*	5.77	30.70	23.22	16.11	5.51	19.392	15.615	39.020
	Gri1	6.13	26.61	22.75	17.47	4.50	19.801	15.651	39.085
m-c	*M9*	5.36	24.06	17.56	19.79	4.65	19.670	15.646	39.213
cum	*Gl1*	4.60	17.82	23.77	12.55	4.01	19.526	15.633	39.042
	Gl4	4.73	19.96	18.08	16.96	4.37	19.620	15.643	39.191
	Gl4[a]	—	—	—	—	—	19.616	15.636	39.193
Finnem	*Fi3*	5.84	20.17	12.46	30.85	3.52	20.146	15.632	39.335
	NBS981	—	—	—	—	—	16.9371	15.4913	36.7213

Rock type symbols as in Tables 2 and 3; NBS891-ratios are the accepted values used by the Univ. of Alberta group (Deb et al. 1989); [a], duplicate analyses; $\lambda(^{238}U) = 1.55125*10^{-10}yr^{1}$; $\lambda(^{235}U) = 9.8485*10^{-10}yr^{-1}$; $\lambda(^{232}Th) = 4.9475*10^{-11}yr^{-1}$

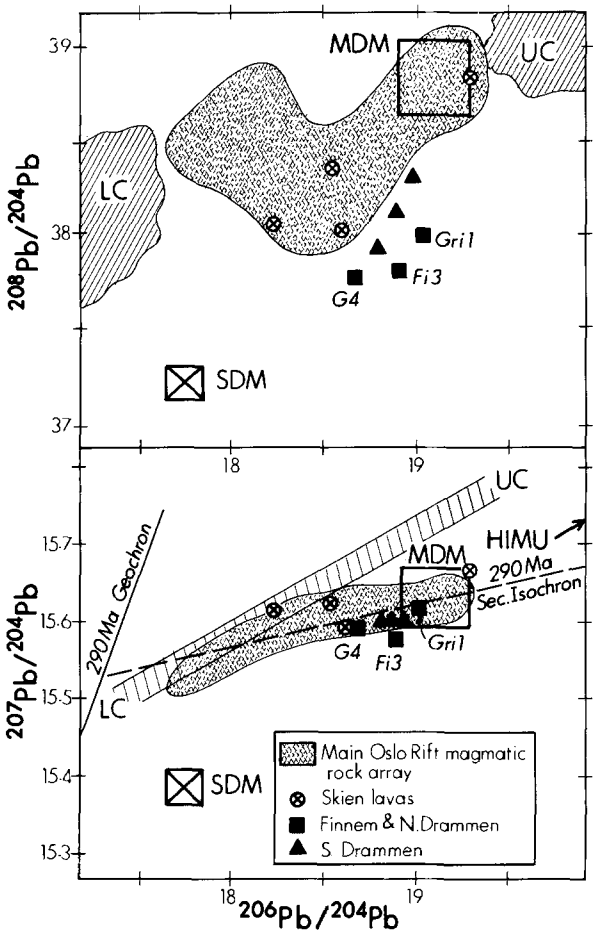

Fig. 8. Initial Pb isotopic relations of Oslo Rift magmatic rocks from Neumann et al. (1988a) and this study. The components *MDM*, *LC* (lower crust), *UC* (upper crust), and *SDM* (strongly depleted mantle at 280 Ma) are discussed by Neumann et al. (1988a). In the $^{207}Pb/^{204}Pb$–$^{206}Pb/^{204}Pb$ diagram the *region with diagonal ruling* represents the range of intermediate crust compositions in SE Norway. The *HIMU* component is from Zindler and Hart (1986)

melting of a lower crust formed by underplating of mantle-derived magmas shortly before or during the early stages of the Permo-Carboniferous magmatic event. A combination of these two processes is also possible, and would be favourable from a heat balance point of view.

The Skien alkali basalts and nephelinites, considered to be the earliest major manifestation of the Oslo Rift magmatism (290 Ma; Sundvoll et al. 1990), are the only magmatic rocks yet observed with a corresponding Sr-Nd isotopic signature (Neumann et al. 1988a, 1990; Anthony et al. 1989). Anthony et al. (1989) postulated that LoNd (low ε_{Nd}; Hart et al. 1986) and alleged HIMU (time integrated high U/Pb; Zindler and Hart 1986) signatures of these alkaline volcanics were related to a mantle metasomatic event associated with the carbonatitic volcanism at Fen 540 Ma. ago (Andersen 1987; Andersen and Taylor 1988). There is, however, no evidence for a HIMU initial Pb signature in the four Skien lavas analyzed (Neumann et al. 1988a). One of the samples plots within the area on the Pb diagrams where the Oslo Rift MDM mantle source plots, whereas the other three lie along mixing arrays from MDM to known crustal compositions in SE Norway (Fig. 8). The Isotopic signatures of the Skien lavas could also be generated by mixing of MDM and an enriched mantle component (EM1; Zindler and Hart 1986). The EM1-component is practically indistinguishable from, lower crust in terms of Sr-Nd-Pb isotopic relations (Zindler and Hart 1986).

A petrogenetic link between the samples from the Finnemarka and northern Drammen batholith and the Skien lavas could involve a common MDM mantle source followed by similar contamination by lower crust prior to emplacement or eruption (Figs. 7–9). Alternatively, the isotopic signatures could have been formed by a combination of MDM and EM1 mantle sources, or by a combination of MDM and EM1 for the Skien lavas and MDM and lower crust for the Finnemarka and northern Drammen batholiths. Significant crustal contamination is much less likely in alkaline mafic volcanics (in particular the silica undersaturated types) than in granites. The two mentioned scenarios, however, seem to have nearly equal probability for the granites.

The samples from the sourthern part of the Drammen granite complex (medium- to coarse-grained and cumulophyric granites) show a significant increase in radiogenic Sr (ε_{Sr} values ranging from + 35 to + 67) relative to the

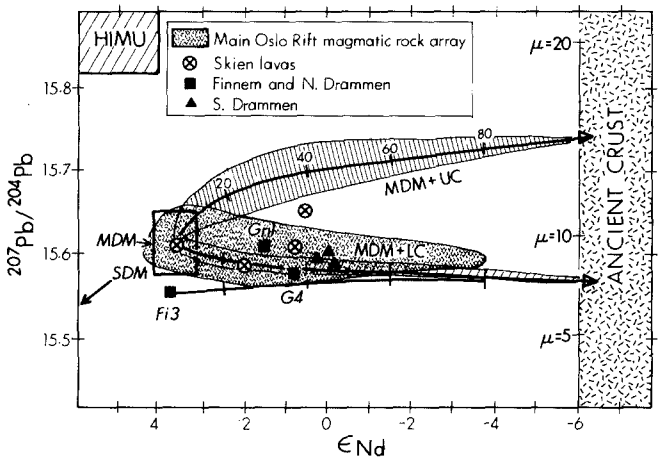

Fig. 9. $^{207}Pb/^{204}Pb$ versus ε_{Nd} (after Neumann et al. 1988a). *Mixing arrays* between *MDM* and *UC* and *LC* (see Fig. 8), using a range of PB abudances of 6 to 50 ppm, and a mixing line between *Fi3* and *LC* are shown

Finnemarka batholith and the northern part of the Drammen batholith. These samples have relatively abundant miarolitic cavities, and a possible explanation for the elevated ε_{Sr} is shallow-level wallrock assimilation or magma-fluid interaction. As shown in Fig. 7, the addition of only 5% of an upper crustal fluid (from Neumann et al. 1988a) to granites with Sr-Nd abundances and isotopic composition like the northern Drammen batholith would be sufficient to increase the ε_{Sr} from 5 to 40. Although extensive crustal anatexis is unlikely at depths less than 10–15 km (Miller et al. 1988) and wallrock xenoliths are absent in the granite complex, it is also possible that shallow-level assimilation of Precambrian and Cambro-Silurian wallrocks affected the isotopic composition close to the southern margin of the batholith.

T_{DM}(Nd) model ages of granitic rocks may be significantly affected by fractionation of monazite and other LREE-minerals, which will markedly increase the Sm/Nd ratio of the melt (Turpin et al. 1990). Monazite is very rare in magmas where Ca-bearing LREE-phases are stable (Parrish 1990) and was not observed in our samples. Titanite, zircon and apatite are the most important REE-bearing minerals in the Drammen and Finnemarka batholiths, and their combined fractionation is not likely to change the Sm/Nd-ratio significantly (e.g. Henderson 1984, Fig. 1.14). The partial melting or fractionation processes that produced the granitic magmas probably did not result in large changes in the Sm/Nd-ratio, because the likely parental magmas or mafic sources, i.e. the Oslo Rift mafic and intermediate rocks, have Sm/Nd-ratios that cover approximately the same ranges as the granites themselves (Neumann et al. 1988a; Anthony et al. 1989). A correlation does exist between the Sm/Nd-ratio and T_{DM}(Nd) (correlation coefficient r = 0.68), but the Nd and Sr initial ratios are also correlated with T_{DM}(Nd) (r = − 0.69 and r = 0.70, respectively). In a strictly qualitative sense we therefore speculate that the model ages represent mixing between sources of different ages (see Arndt and Goldstein 1987). The model ages for the Finnemarka and northern Drammen samples ranging from 602 to 764 Ma may indicate mixing of Precambrian mantle (MDM; Mearns et al. 1986) and crustal sources with a younger component, possibly related to a metasomatic event associated with the carbonatitic magmatism in the Fen region at 540 Ma (Anderson and Taylor 1988). The Skien lavas have a similar T_{DM}(Nd) model age range of 620 to 810 Ma (Anthony et al. 1989). The greater Nd model ages of 900 to 1220 Ma in the sourthern part of the Drammen batholith may be caused by decreasing importance of the relatively young (metasomatic?) mantle component and increasing contributions of Precambrian upper crustal material.

Loiselle and Wones (1979), Collins et al. (1982) and Whalen et al. (1987) described the chemical characteristics of anorogenic (A-type) granites, including their dominantly metaluminous or peralkaline compositions. Peraluminous granites, however, are most commonly associated with compressional tectonic settings, and anatexis of metasedimentary material is generally considered the most common origin of such magmas (Chappel and White 1974; Le Fort 1975; White and Chappel 1988). In a regional study of a range of Mesozoic and Tertiary peraluminous and metaluminous granites in the western United States, Farmer and DePaolo (1983, 1984) found that the peraluminous types have systematically lower ε_{Nd} (− 10 to − 30) and higher ε_{Sr} (+ 80 to + 240) than the metaluminous types (0 to − 20 and 0 to 150, respectively), and they concluded that the former were derived mainly from crustal Precambrian sources.

In spite of the anorogenic nature of the Oslo Rift, large volumes of mildly peraluminous granites occur along with the metaluminous to peralkaline syenites and granites of the "common Oslo Rift magmatic series". Major portions of these peraluminous granites in the central part of the rift retain mantle isotopic signatures, with some samples similar isotopically to the earliest extruded nephelinites and alkali basalts and the MDM mantle source proposed for the Oslo Rift. Therefore, fractionation of mantle-derived mafic melts, as well as direct partial melting of mafic rocks in the crust, should be evaluated as possible petrogenetic scenarios.

Liquidus phase relations and major element modelling of fractionation and partial melting

Least squares, major element, mass balance calculations were carried out in order to assess the feasibility of deriving melts of Drammen granite composition by: (1) fractional crystallization of parental melts similar in composition to the Skien alkaline volcanics and the Vestfold alkaline to tholeiitic basalts and (2) partial melting of lower crustal gabbros. The petrogenetic models presented next do not provide unique solutions, but illustrate the general plausibility of the proposed melting and fractionation processes.

At low pressure, the join olivine-plagioclase-clinopyroxene represents a thermal divide between alkaline and tholeiitic basaltic melts. Experimental studies of the liquidus phase relations in the CaO-MgO-Al_2O_3-SiO_2-system (Presnall et al. 1978, 1979) indicate that at pressures above ≈ 4 kbar alkali olivine basaltic melts can

yield quartz tholeiites by fractionation of assemblages involving aluminous clinopyroxene. Johnson and Rutherford (1990 and in preparation) investigated the liquidus phase relations of an alkaline transitional basalt and a basanite between 1 bar and 5 kbar pressure, and found that clinopyroxene was the liquidus phase followed by kaersutitic amphibole for both compositions. Zen (1986) demonstrated that the ASI of a felsic magma can be significantly increased by the subtraction of low-ASI phases like clinopyroxene and hornblende, or decreased by fractionation of high-ASI minerals like biotite and muscovite.

Clinopyroxene was probably a major fractionating phase in the alkaline to tholeiitic basaltic magmas of the Olso Rift, because it is the dominant phenocryst phase throughtout the Skien lava statigraphy and at the lower B1 stratigraphic level at the Vestfold lava plateau (Fig. 1; Segalstad 1979; Neumann et al. 1990). The elongate gravity anomaly along the Oslo Rift axis indicates that large amounts of dense material, possibly cumulates and/or residues from partial melting, are present in the lower crust (10–32 km depth; Ramberg 1976; Wessel and Husebye 1987; Olsen et al. 1987; Neumann et al. 1986 and in preparation). Only one occurrence of xenoliths from this level is known (Krokskogen lava plateau; Neumann et al. 1988b). The only xenolith lithology encountered is olivine clinopyroxenite meta-cumulate. Based on studies of fluid inclusions, the minimum pressure of origin of these xenoliths is 5.5–6 kbar. Another potentially fractionating phase, kaersutitic amphibole, is also present as phenocrysts in the Skien lavas and in many small Permian gabbroic intrusions (Segalstad 1979; Neumann et al. 1985). Apart from clinopyroxene and kaersutitic amphibole, independent control on the residual or crystallizing phases is rather poor. This is due to the large compositional range from parent to daughter compositions, and the absence of obvious intermediate products.

Initially, various Oslo Rift larvikites and rhomb porphyries were used as intermediate compositions in the fractionation modelling. The evolution from the silica undersaturated Skien basalts or the near silica saturated Vestfold basalts to the near silica saturated larvikites give acceptable solutions with 50–80% fractionation of mainly cpx (60–80% of the crystallizing assemblage), and minor amounts of olivine, spinel, titanite or amphibole. Regardless of the choice of fractionating assemblage, the alkali content of the larvikites is too high relative to Al, Si, Fe and Mg to produce any of the biotite granites. Good solutions are obtained, however, by using realistic residual assemblages in single stage models. Four of these models, using the clinopyroxene compositions from the cumulate xenoliths at Krokskogen and a Skien lava phenocryst, are shown in Table 6.

Beard and Lofgren (1989, 1991) compared the compositions of silicic melts derived in H_2O-saturated and H_2O-undersaturated experiments on natural basalts. In terms of Al_2O_3 and FeO versus SiO_2 the samples from the Drammen batholith fall into the compositional range of melts in equilibrium with anhydrous, granulitic residues (plag + cpx ± opx ± ol + mt + il + ap) at 1–7 kbar pressure. Amphibole-bearing residues are generally formed under H_2O-saturated or near saturated conditions and are accompanied by melts with considerably higher Al_2O_3-content at pressures of 3–7 kbar (> 15.5% and > 17% at 70% and 75% SiO_2, respectively). The high F-content of the Drammen and Finnemarka magmas, however, might favour the stabilization of amphibole and biotite in residues from partial melting in the lower crust. The fractionating assemblages obtained in the major element modelling are in any case in general agreement with the residues found in the melting experiments.

Major element mass balance calculations were also attempted for a possible internal differentiation of the Drammen granite complex. The rock types with low-and intermediate-silica contents were used as parent compositions and the medium-grained granite and the aplitic porphyry were chosen as daughter compositions. The late- to post-magmatic albitization of the latter, however, invariably results in solutions involving fractionation of K-feldspar and biotite combined with assimilation of albitic plagioclase.

In the central granitic stock of the Glitrevann Cauldron between the Drammen and Finnemarka complexes Jensen (1985) observed a regular decrease in the peraluminousity of the granites that is positively correlated with the degree of differentiation. This can be explained by the combined fractionation of feldspars and biotite in a comagmatic suite. Within the Drammen granite complex, however, the variation of SiO_2 (degree of differentiation) is largely decoupled from the variations of the ASI $= Al_2O_3/(CaO + Na_2O + K_2O)$ and the $Al_2O_3/(Na_2O + K_2O)$ ratios (Figs 3 and 4). Although hydrothermal overprinting (Na-K-exchange, albitization) may slightly affect the position of the medium-to fine-grained granite and aplitic porphyry samples in Fig. 4, this decoupling, especially between the rapakivi granite and the fine-grained porphyry, indicate that the different rock types are not strictly comagmatic.

Trace element constraints

The major element mass balance models of Table 6 have been evaluated using trace element data in Table 7. The wide range from parental compositions of silica undersaturated to quartz tholeiitic basalts to the produced biotite granites lead to considerable uncertainties in the trace element modelling. In fractional crystallization modelling, in particular, the choice of partitioning coefficients becomes critical to the results, and the large range in melt compositions lead to large variations in the partition coefficient for a mineral that crystallizes over a significant melt compositional range. The partitioning coefficients in Table 7 are chosen based on the assumption that clinopyroxene is an early crystallizing phase (weakly alkaline, mafic melt composition) and that the other minerals crystallize mainly from intermediate to silicic melts. In the partial melting modelling, all of the partitioning coefficients are applicable to intermediate to silicic melts.

The observed concentrations of most of the trace elements are in reasonably good agreement with the model predictions. Since the presented models clearly represent large simplifications, however, there are also

Table 6. Results from least squares mass balance modelling

		SiO_2	TiO_2	Al_2O_3	FeO	MnO	MgO	CaO	Na_2O	K_2O	P_2O_5
Parents: alk (Skien)		45.2	3.07	11.4	12.3	0.20	9.57	11.3	2.23	1.87	0.38
F13 (Vestfold)		44.3	4.81	9.46	12.2	0.16	8.10	11.6	1.70	1.92	0.75
FA4 (Vestfold)		52.5	4.90	10.4	8.81	0.13	5.41	10.3	2.26	1.90	0.60
Daughter: c(Drammen)		76.2	0.31	13.8	1.39	0.03	0.23	0.68	3.22	5.13	0.05
Subtracted phases:											
Clinopyrox.:	cpl	49.4	1.26	5.29	7.52	0.14	14.7	20.6	0.67	—	—
	cp2	47.1	2.6	6.3	7.6	—	12.4	22.2	0.5	0.1	—
Amphibole:	am	39.1	7.0	11.9	11.4	0.3	13.3	11.5	2.8	1.0	—
Plagioclase	pl1	55.5	—	27.9	0.52	—	0.02	10.1	5.35	0.62	—
	pl2	58.1	—	26.4	0.19	—	0.03	7.84	6.48	1.10	—
	pl3	53.0	—	29.3	0.84	—	—	12.3	4.21	0.13	—
Biotite:	bi	39.8	1.87	11.5	14.0	—	16.5	—	—	10.3	—
Ti-magnetite:	mt1	—	19.4	1.39	71.5	—	2.30	—	—	—	—
	mt2	—	6.99	3.60	75.0	—	7.18	—	—	—	—
	mt3	—	26.8	2.31	64.8	—	1.90	—	—	—	—
Ilmenite	ilm	0.51	50.0	—	47.4	—	0.46	0.71	—	—	—
Apatite:	ap	—	—	—	0.03	0.01	0.02	55.9	—	—	42.0

	Parent	Residual assemblage	Melt fraction (% daughter)	Σ(residuals)^2
Model 1:	alk	40.9 cpl + 13.4 am + 21.8 pl1 + 14.1 bi + 9.1 mtl + 0.7 ap	8.3	0.22
Model 2:	alk	35.4 cp2 + 29.9 am + 14.4 pl1 + 11.4 bi + 8.1 mt2 + 0.7 ap	13.6	0.25
Model 3:	F13	53.7 cp1 + 18.9 pl2 + 10.2 bi + 10.9 mt3 + 3.8 ilm + 2.4 ap	14.1	0.05
Model 4:	FA4	59.7 cpl + 20.9 pl3 + 5.7 mt3 + 11.1 ilm + 2.7 ap	38.0	0.16

Values in weight percent; alk, average of Skien alkali basalt analyses S49, S55, and S66 (normative ne + ol, Anthony et al. 1989); F13 (normative hy) and FA3 (normative qz + hy), analyses of Vestfold lavas from Neumann et al. (1990); c, average of coarse grained granite analyses G4 and Gri1 from the northern part of the Drammen batholith; cp1, average of clinopyroxenes in cumulate xenoliths from Krokskogen (Neumann et al. 1988b); cp2 and am, phenocryst analyses no. 138 and 472 in Skien lavas (Segalstad 1979); bi, biotite in G5 (Table 1); p11, p12, and p13, average of analyses no. 4 and 5, analysis 4, and analysis 5 in Deer et al. (1966); mt1, mt2, and mt3, analyses no. 7, 6, and 8 in Deer et al. (1962); ap, analysis no. 3 in Deer et al. (1966)

Table 7. Trace element modelling using melt fractions and residual mineral assemblages of Table 6

	Mineral-melt partitioning coefficients						Model 1		Model 2		Model 3		Model 4		Observed
	cpx	amph	plag	biot	oxide	ap	Ra	Eq	Ra	Eq	Ra	Eq	Ra	Eq	Drammen
Rb	0.01	0.01	0.04	2.0	0.02	—	274	133	219	140	203	133	101	99	233
Sr	0.3	0.4	6.0	0.4	1.0	8	138	472	438	617	265	624	397	582	101
La	0.2	2.0	0.3	0.3	0.5	20	113	69	51	48	129	101	80	76	46
Sm	0.8	4.0	0.2	0.4	0.9	54	3.2	6.5	1.2	4.8	2.7	9.4	4.7	8.2	4.6
Eu	0.7	3.5	2.0	0.3	0.6	27	0.8	1.8	0.5	1.5	1.7	3.3	2.1	2.8	0.6
Tb	0.7	5.0	0.2	0.4	0.8	20	0.4	0.6	0.1	0.4	1.4	1.5	1.2	1.2	0.5
Lu	0.8	4.0	0.06	0.7	0.4	17	0.2	0.2	0.1	0.1	0.4	0.4	0.3	0.3	0.4
Th	0.03	0.2	0.04	0.3	0.2	—	41	25	25	18	49	37	16	15	29
U	0.03	0.4	0.04	0.3	0.3	—	10	5	6	4	9	7	4	4	6
Rb	0.03						274	134	214	136	199	129	100	98	233
Sr	0.5						116	451	381	588	213	589	353	554	101
La	0.6						74	56	38	43	85	82	64	65	46
Sm	2.7						0.5	4.3	0.3	3.6	0.4	5.2	1.6	5.8	4.6
Eu	1.9						0.2	1.4	0.2	1.2	0.4	2.3	0.5	1.7	0.6
Tb	2.5						0.1	0.4	0.03	0.3	0.2	0.8	0.4	0.7	0.5
Lu	2.3						0.02	0.1	0.02	0.1	0.1	0.2	0.1	0.2	0.4
Th	0.3						31	15	21	13	37	24	14	12	29
U	0.3						7	4	5	3	7	5	4	3	6

The partitioning coefficients are based on the compilations by Cox et al. (1979), Henderson (1983), and Lemarchand et al. (1987). The large range of melt compositions lead to considerable uncertainties in the partition coefficients. In the upper half of the table it is assumed that clinopyroxene crystallizes mainly from mafic melts and the other minerals mainly from intermediate and silicic melts. The lower half of the table refers to the partial melting scenario, and all of the partition coefficients are applicable to intermediate to silicic melts. The model concentrations and the concentrations observed in samples from the northern part of the Drammen batholith (average of Gri1, G4, and G7) are in weight ppm. Ra, Rayleigh fractionation process; Eq, equilibrium fractionation process

important discrepancies. None of the models are distinctly favoured relative to the others. The modelled Rb and Sr concentrations are generally lower and higher than the observed values, respectively, possibly indicating that feldspar fractionation was more extensive than predicted. Plagioclase is the only feldspar mineral involved in the models, but the general covariation of Sr and Ba within the Drammen granite suite may point to combined fractionation of plagioclase and alkali feldspar. The observed concentrations of Sm, Eu, Tb, Th, and U are in good agreement with the model predictions, but the observed LREE and HREE are generally lower and higher than the model predictions, respectively. A very small amount of monazite and/or allanite crystallization as minute inclusions in biotite and oxides in granitic magmas can cause large LREE-depletion and may be impossible to recognize by major element mass balance calculations and standard petrographic techniques (Miller and Mittlefehldt 1982, 1984; Mittlefehldt and Miller 1983; Michael 1988; Bacon 1989). The elevated HREE-contents could be caused by selective assimilation of garnet from crustal sources or by HREE-fluoride complexing and segregation of the type described by Bandurkin (1961), Mineyev (1963), Balashov and Krigmann (1975), Harris (1981), and Taylor et al. (1981). The latter mechanism would explain the enrichment of both F and HREE in the medium- to fine-grained granite and aplitic porphyry.

Although the late-stage hydrothermal overprinting seen as albitization in the medium-grained granite and aplitic porphyry clearly may affect trace elements also, the regular Rb-Sr-Ba-Eu variation within the Drammen granite suite indicate that the different rock types have undergone variable degrees of feldspar and mica fractionation. The depletion of Zr and rare earth elements from the cumuloporphyritic granite and the fine-grained porphyry to the medium- to fine-grained granite and aplitic porphyry is consistent with fractionation of zircon, titanite, and apatite. The high concentrations of elements like Y and Nb and F in the Drammen and Finnemarka complexes are characteristic of within-plate granites and A-type granites (collins et al. 1982; Pearce et al. 1984; Whalen et al. 1987).

Magmatic and residual infrastructure of the crust

Husebye and Ramberg (1978) summarized the geophysical data for the Oslo Rift and Ramberg (1976) and Wessel and Husebye (1987) provided detailed discussions of the large positive gravity anomaly extending over the entire rift axis and considerably beyond the rift boundaries in the east-west direction. Ramberg (1976) ascribed the gravity anomaly to the combined effect of crustal thinning and dense material in the lower to intermediate crust, whereas Wessel and Husebye (1987) located a 10 km thick and 100 km wide causative body with a density contrast of 60 kg/m^3 in the upper part of the lower crust (10–20 km depth). A revised model for the crustal mass distribution based on a wider range of geophysical (gravimetric, seismic, aeromagnetic and heat flow) and petrological data is presented by Olsen et al. (1987) and Neumann et al. (in preparation). This model also involves a 10 km thick and 100 km wide body with a similar density contrast, but locates it immediately above the Moho, rather than in the upper part of the lower crust.

The plate-like Drammen batholith, with its 3 km thickness (Ramberg 1976), has a volume of about 60 km^3/km along the NNE-SSW trending rift axis. The density of the granite (2610 kg/m^3) is significantly lower than that of the lower crustal body (3130–3400 kg/m^3; Ramberg 1976; Neumann et al. 1986) which has a volume of about 1000 km^3/km along the rift axis. Therefore, the weight fraction of the Drammen granite is about 5% of the dense crustal body. If this body represents clinopyroxene-rich cumulates and/or partial melting residues (Neumann et al. 1986, 1988b), the part of it underlying the Drammen complex is twice to eight times the size required according to the mass balance calculations of Table 6. The northern part of the southern rift segment is dominated by the Drammen and Finnemarka batholiths, allowing for more granitic material at depth and a considerable portion of additional cumulates or residues within the total mass of the dense body.

If the mafic magma that intruded the lower crust under the Drammen and Finnemarka complexes was of the same parentage as the earliest erupted basalts (the stratigraphically lowest B_1 lavas), a volume comparison may illustrate the early processes ultimately leading to granitic magmas by partial melting or crystal fractionation from gabbroic parental material. The preserved total thickness of the alkaline Skien basalts is 1.5–2 km, but the thickness and alkalinity of the basalts of the B_1 stratigraphic level decreases northwards to 1500–180 m at the Vestfold lava plateau and less than 30 m north of Oslo (Ramberg 1976; Ramberg and Larsen 1978; Segalstad 1979; Neumann et al. 1990). The extent and distribution of Permian volcanic dikes in the Precambrian rocks outside the Oslo Rift indicate that the lava cover exceeded the graben area by about a factor of two (Ramberg and Larsen 1978). If the early basalt pile was 1 km thick and had a 100 km east-west extension its volume of 100 km^3/km along the rift axis would be only 10% of the dense crustal body. Because dense mafic magmas may be prevented from penetrating the crust in periods of low to moderate tensional stresses in the crust and uppermost mantle (e.g. Neumann 1980; Herzberg et al. 1983), such a low percentage is not unexpected. The larvikite-dominated batholiths emplaced in the southern rift segment at an early stage of the magmatic evolution are also evidence for a considerable magmatic crustal infrastructure associated with the early basaltic volcanism.

Position of peraluminous granites in the rift and in the magmatic evolution

The uniformly silicic nature and relatively small amount of Precambrian crustal contamination in the peraluminous granites may be explained in part by a refractory nature of the lower crust in the central part of the Oslo Rift. Killeen and Heier (1975) pointed out the geographical coincidence between the Drammen and Finnemarka batholiths and a NNW-trending belt of late Precambrian granite batholiths (Fig. 1). They suggested

that the Drammen and Finnemarka batholiths were formed by crustal melting and reworking of these older granites. If the Precambrian granites were formed by melting of the lower crust (Wilson 1982; Pedersen and Maaløe 1990), however, it is likely that the lower crust became more refractory and less prone to partial melting in Permian time. The low $^{208}Pb/^{204}Pb$ ratios of Permian magmatic rocks and mineralizations from the central part of the rift, and in particular from the Drammen and Finnemarka complexes, may indicate a time-integrated Th-depletion in the lower crust and/or mantle lithosphere in this area.

Extensive crustal anatexis is unlikely to occur at depths less than 10–15 km, even under extreme geothermal conditions (Miller et al. 1988). Apart from the high radiogenic Sr values of the samples from the southern part of the Drammen granite, the isotopic signatures of the analysed Drammen and Finnemarka samples generally point to lower crustal sources for the observed contamination (Figs. 7–9). The elevated radiogenic Sr in the south may be caused by magma interaction with upper crustal fluids or wallrock xenoliths close to the southern margin of the batholith.

A simplified N-S (SSW-NNE) crustal section along the rift axis is illustrated in Fig. 10. In accordance with the model of Olsen et al. (1987) and Neumann et al. (in preparation), a 10 km thick layer of dense cumulates and/or residues is shown immediately above the Moho. In the central part of the rift some of this material is also indicated in the uppermost part of the lower crust. If the lower crust in this area is unusually refractory and dense,

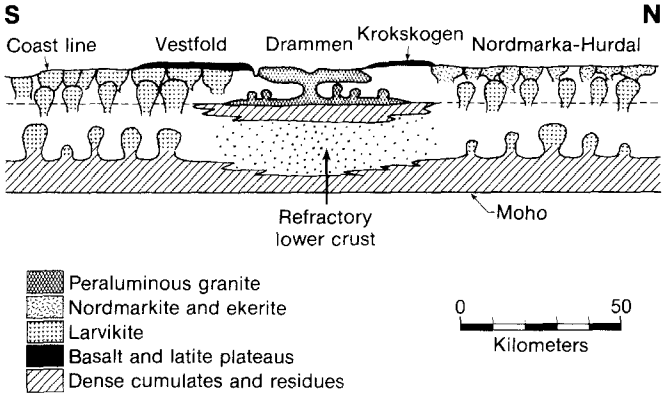

Fig. 10. Simplified S-N (SSW-NNE) crustal section along the rift axis. The position of the profile is shown in Fig. 1. The vertical scale is slightly exaggerated, and the topographic relief is greatly exaggerated and simplified. The main elements of the crustal structure are: upper-lower crust boundary at $\approx$ 10 km depth, Moho at $\approx$ 30–35 km depth (Wessel and Husebye 1987) and a $\approx$ 10 km thick high-density body immediately above Moho (Olsen et al. 1989; Neumann et al. in prep.). The refractory and dense nature of the lower crust and a correspondingly low density of the upper crust beneath the central part of the rift are inferred from the location of a belt of late Precambrian granites (see Fig. 1), the small amounts of intermediate intrusive rocks in the central part of the rift, and the isotopic composition of the Drammen and Finnemarka batholiths. An implication of the postulated high-density lower crust under the central part of the rift is that density filtering of mafic melts near the Moho was less efficient. Therefore, dense cumulates are also indicated near the top of the lower crust in this region

the crust-mantle boundary is not expected to be a completely efficient density barrier, and a larger proportion of relatively primitive melt is expected to reach shallower levels, possibly resulting in more extensive magma accumulation at the boundary between the lower and the upper crust (10 km depth). This boundary probably also had a more distinct density contrast in the central part of the rift than to the north and south. A well-developed density barrier at about 10 km depth may explain the uniformly silicic composition of the Drammen and Finnemarka complexes and the deficiency of intermediate magmatic rocks in the central part of the rift. Such an upper crustal density filtering effect will apply regardless of whether the silicic magma generation occurred by fractionation or partial melting.

The large larvikite complexes in the sourthern part of the rift indicate a denser upper crust allowing intermediate magmas to rise to shallow level. The crustal density distribution in the northern rift segment may have been intermediate between those of the central peraluminous granite region and the southern larvikite region. This allowed intermediate (larvikitic) magmas into the upper crust but forced most of them to further differentiate to nordmarkites and ekerites prior to shallow level intrusion.

The earliest stage of the magmatism in the Oslo Rift is characterized by relatively high tensional stress and fissure eruptions of the B_1 Skien and Vestfold basalts. The high tensional stress and basaltic eruptions in the southwest were either accompanied by more isotropic stress conditions in the Drammen and Finnemarka area and/or followed by such conditions, causing upper crustal density filtering and accumulation of basaltic magma. Differentiation of these melts to form intermediate, and possibly granitic, magmas would release a considerable amount of latent heat. If the differentiated, intermediate melts were prevented from ascending to shallower levels, the result would be a significant accumulation of heat. Extensive partial melting of already solidified rocks (cumulates and crystallized mafic and intermediate melts) would therefore be expected in this region. Successive magma injections forming sill-like magma chambers at the base of the preceeding, and largely solidified and stratified, intrusions would provide heat sources for partial melting, possibly of the most differentiated rocks in the overlying magmatic sequence (see also Creaser et al. 1991). Partial melting of a somewhat differentiated mafic to intermediate rock will also provide a mechanism of F-enrichment, as F partitions strongly into the melt (e.g. Fuge 1977).

Conclusions

The radiogenic isotope signatures of the Drammen and Finnemarka batholiths dictate that most of the magmas were generated either by fractional crystallization of mantle-derived alkaline to tholeiitic basaltic magmas or by water-undersaturated partial melting of crustal gabbroic or intermediate rocks of broadly similar composition emplaced immediately prior to or during the Permo-Carboniferous magmatic episode. Liquidus phase relations and mass-balance constraints are consistent with

either of these mechanisms, but the partial melting scenario is favoured on the basis of heat balance considerations. The lack of igneous rocks of intermediate composition associated with the peraluminous granites point to an efficient upper crustal density filtering. Considerable amounts of heat would be accumulated in this region if differentiated, intermediate magmas were not allowed to rise into the upper crust. Successive magma injections would promote partial melting of already solidified mafic to intermediate melts and cumulates.

The efficient upper crustal density filtering effect probably resulted from earlier extensive intracrustal differentiation indicated by the NNE-SSW trending belt of late Precambrian granites, geographically aligned with the Finnemarka and Drammen batholiths. The modest amount of Precambrian crustal contributions to the Drammen and Finnemarka batholiths may also be explained by a refractory lower crust following the 0.9 Ga granite formation event.

The contribution of Precambrian crustal material is insignificant or minor in the Finnemarka batholith and northern part of the Drammen batholith. The Sr-Nd-Pb isotopic ratios point to a lower crustal contaminant with time integrated depletion of Rb, Nd, U, and in particular Th. The samples from the southern part of the Drammen batholith have strongly elevated ε_{Sr} (+ 35 to + 67), but the Nd and Pb isotopic ratios overlap with the samples from the northern part of the batholith. The high radiogenic Sr-content is most likely caused by a combination of shallow level wallrock assimilation and/or magma-fluid interaction.

The Skien alkali basalts are the only other Oslo Rift magmatic rocks within the low ε_{Sr} area defined by the Finnemarka and northern Drammen samples. This may reflect a petrogenetic link, e.g. in the form of remelting of early emplaced lower crustal gabbroic rocks of Skien basaltic nature. The similarity, however, may also be a result of the mixing relationships MDM—EM1 and MDM—lower crust for the Skien lavas and the peraluminous granites, respectively.

In spite of their peraluminous nature, the biotite granites also have certain characteristics in common with A-type and within-plate granites, in particular in the form of high contents of F, Nb and Y and hypersolvus feldspars. The peralumious chemistry was most likely acquired by fractionation (in the form of partial melt separation from the solid residue and/or fractional crystallization) of low-ASI minerals like clinopyroxene and amphibole (Zen 1986). The major and trace element chemical variation within the Drammen granite suite indicate that the different rock types underwent additional and variable fractionation of plagioclase, alkali feldspar, mica, and accessory phases.

Acknowledgements. Most of the work by RGT was carried out at the Norwegian Institute of Technology, and was funded by grants from the Royal Norwegian Council for Scientific and Industrial Research to P. M Ihlen and F.M. Vokes and the Norwegian Research Council for Science and the Humanities to RGT. Norsk Hydro Ltd. financially supported the geological mapping program. The isotope work by ADB at the University of Alberta was supported by a Natural Sciences and Engineering Research Council of Canada operating grant to R. St. J. Lambert. Discussions with and advice from many people including T. Chacko, P. M. Ihlen, R. St. J. Lambert, B. T. Larsen, M. Martinsen, E.-R. Neumann, A. D. Smith, B. Sundvoll, F. M. Vokes, and T. Vrålstad are greatly appreciated. R. W. Luth provided a detailed and very helpful critique of an early version of the paper. Further reviews and suggestions by E. Anthony, E.-R. Neumann, P. J. Patchett, and G. Stenstrop also contributed to important clarifications and corrections.

References

Allegre CJ, Hart SR, Minster JF (1983) Chemical structure and evolution of the mantle and continents determined by inversion of Nd and Sr isotopic data. II. Numerical experiments and discussion. Earch Planet Sci Lett 37:191–213

Andersen T (1987) Mantle and crustal components in a carbonatite complex, and the evolution of carbonatite magma: REE and isotopic evidence from the Fen complex, southeast Norway. Chem Geol 65:147–166

Andersen T, Taylor PN (1988) Pb isotope chemistry of the Fen carbonatite complex, S.E. Norway: age and petrological implications. Geochim Cosmochim Acta 52:209–216

Anthony EY, Segalstad TV, Neumann E-R (1989) An unusual mantle source region for nephelinites from the Oslo Rift, Norway. Geochim Cosmochim Acta 53:1067–1076

Arndt NT, Goldstein SL (1987) Use and abuse of crust-formation ages. Geology 15:893–895

Bacon CR (1989) Crystallization of accessory phases in magmas by local saturation adjacent to phenocrysts. Geochim Cosmochim Acta 53:1055–1066

Beard JS, Lofgren GE (1989) Effect of water on the composition of partial melts of greenstone and amphibolite. Science 244:195–197

Beard JS, Lofgren GE (1991) Dehydration melting and water-saturated melting of basaltic and andesitic greenstones and amphibolites at 1, 3, and 6.9 kb. J Petrol 32:365–401

Balashov YA, Krigman LD (1975) The effect of alkalinity and volatiles on rare-earth separation in magmatic systems. Geokhimiya 12:1885–1890

Bandurkin GA (1961) Behavior of the rare earths in fluorine-bearing media. Geokhimiya 2:143–149

Barth TFW (1954) Studies on the igneous rock complex of the Oslo Region. XIV. Provenance of the Oslo magmas. Skr Norske Vitensk-Akad i Oslo, I. Mat-naturv Kl No 4

Barth TFW (1962) Theoretical petrology, 2nd edn. Wiley, New York

Bjørlykke A, Ihlen PM, Olerud S (1987) Metallogeny and lead isotope data from the Oslo Paleorift. Tectonophysics 178:109–126

Chappel BW, White AJR (1974) Two contrasting granite types. Pacific Geol 8:173–174

Colby JW (1968) Quantitative microprobe analysis of thin insulating film. Adv X-ray Anal 10:287–305

Collins WJ, Beams SD, White AJR, Chappell BW (1982) Nature and origin of A-type granites with particular reference to southeastern Australia. Contrib Mineral Petrol 80:189–200

Cox KG, Bell JD, Pankhurst RJ (1979) The interpretation of igneous rocks. George Allen & Unwin, London

Creaser RA, Price RC, Wormald RJ (1991) A-type granites revisited: assessment of a residual-source model. Geology 19:163–166

Czmanske GK (1965) Petrological aspects of the Finnemarka granite complex, Oslo area, Norway. J. Geol 73:239–322

Deb M, Thorpe RI, Cumming GL, Wagner, PA (1989) Age, source, and stratigraphic implications of Pb isotopic data for conformable, sediment hosted base metal deposits in the Proterozoic Aravalli-Dehli orogenic belt, northwestern India. Precambrian Res 43:1–22

Deer WA, Howie RA, Zussman J (1962) Rock-forming minerals, vol. 5, Non-silicates. Longman, London

Deer WA, Howie RA, Zussman J (1966) An introduction to the rock-forming minerals. Longman, London

DePaolo DJ (1981) Neodymium isotopes in the Colorado Front Range and the crust-mantle evolution in the Proterozoic. Nature 291:193–196

Dickin AP (1981) Isotope geochemistry of Tertiary igeneous rocks from the Isle of Skye, Scotland. J Petrol 22:155–189

Ellis DJ, Thompson AB (1986) Subsolidus and partial melting relations in the quartz-excess CaO-MgO-Al_2O_3-SiO_2-H_2O system under water-excess and water-deficient conditions to 10 kbar: some implications for the derivation of peraluminous melts from mafic rocks. J Petrol 27:91–121

Farmer GL, DePaolo DJ (1983) Origin of Mesozoic and Tertiary granite in the western United States and implications for pre-Mesozoic crustal structure, 1. Nd and Sr isotopic studies in the geocline of the northern Great Basin. J Geophys Res 88, 3379–3401

Farmer GL, DePaolo DJ (1984) Origin of Mesozoic and Tertiary granite in the western United States and implications for pre-Mesozoic crustal structure, 2. Nd and Sr isotopic studies of unmineralized and Cu- and Mo-mineralized granite in the Precambrian craton. J Geophys Res 89, 10141–10160

Fuge R (1977) On the behaviour of fluorine and chlorine during magmatic differentiation Contrib Mineral Petrol 61:245–249

Gaut A (1981) Field relations and petrography of the biotite granites of the Oslo region. Norges Geol Unders 367:39–64

Harris NBW (1981) The role of fluorine and chlorine in the petrogenesis of a peralkaline complex from Saudi Arabia. Chem Geol 31:303–310

Hart SR, Gerlach DC, White WM (1986) A possibly new Sr-Nd-Pb mantle array and consequences for mantle mixing. Geochim Cosmochim Acta 50:1551–1557

Heltz RT (1976) Phase relations of basalts in their melting ranges at p_{H_2O} = 5 kbar. Part II. Melt compositions. J Petrol 17:139–193

Henderson P (1982) Inorganic geochemistry. Pergamon Press, Oxford

Henderson P (1984) General geochemical properties and abundances of the rare earth elements (Ch. 1). In: Henderson P (ed) Rare earth element geochemistry. Elsevier, Amsterdam

Herzberg CT, Fyfe WS, Carr MJ (1983) Density constraints on the formation of the continental Moho and crust. Contrib Mineral Petrol 84:1–5

Hildreth W (1981) Gradients in silicic magma chambers: Implications for lithospheric magmatism. J Geophys Res 86:10153–10192

Husebye ES, Ramberg IB (1978) Geophysical investigations. In: Dons JA, Larsen BT (eds) The Oslo Paleorift. A review and guide to excursions. Norges Geol Unders 337:41–53

Ihlen PM, Trønnes R, Vokes FM (1982) Mineralization, wallrock alteration and zonation of ore deposits associated with the Drammen granite in the Oslo Region, Norway. In: Evans AM (ed) Metallization associated with acid magmatism. John Wiley and Sons: pp 111–136

Jacobsen SB, Raade G (1975) Rb-Sr whole rock dating of the Nordagutu granite, Oslo Region, Norway. Norsk Geol Tidsskr 55:171–178

Jacobsen SB, Wasserburg GJ (1978) Nd and Sr isotopic study on the Permian Oslo Rift. In Zartmann RE (ed) Short papers of the Fourth International Conference on Geochronology, Cosmochronology, and Isotope Geology, US Geol Surv Open File Rep 78–701:194–196

Jacobsen SB, Wasserburg GJ (1984) Sm-Nd isotopic evolution of chondrites and achondrites, 2. Earth Planet Sci Lett 67:137–150

Jensen IS (1985) Geochemistry of the central granitic stock in the Glitrevann cauldron within the Oslo Rift, Norway. Norsk Geol Tidsskr 65:201–216

Johnson MC, Rutherford MJ (1990) Low pressure crystal fractionation of transitional and silica-undersaturated magmas. Eos Trans Am Geophys Union 71:1712

Killeen PG, Heier KS (1975) A uranium and thorium enriched province of the Fennoscandian Shield in southern Norway. Geochim Cosmochim Acta 39:1515–1524

Le Fort P (1975) Himalaya: the collided range. Present knowledge of the continental arc. Am J Sci 275A:1–44

Lemarchand F, Villemant B, Calas G (1987) Trace element distribution coefficients in alkaline series. Geochim Cosmochim Acta 51:1071–1081

Loiselle MC, Wones DR (1979) Characteristics and origin of anorogenic granites. Geol Soc Am Abstr with Progr 11:486

Mahood GA (1981) Chemical evolution of a Pleistocene rhyolitic center: Sierra La Primavera, Jalisco, Mexico. Contrib Mineral Petrol 77:129–149

Manning DAC (1981) The effect of fluorine on liquidus phase relationships in the system qz-ab-or with excess water at 1 kb. Contrib Mineral Petrol 76:206–215

Mearns EW, Andersen T, Mørk MBE, Morvik R (1986) $^{143}Nd/^{144}Nd$ evolution in depleted Baltoscandian mantle. Terra Cognita 6, 247

Michael PJ (1988) Partition coefficients for rare earth elements in mafic minerals of high silica rhyolites: the importance of accessory mineral inclusions. Geochim Cosmochim Acta 52:275–282

Miller CF, Mittlefehldt, DW (1982) Depletion of light rare-earth elements in felsic magmas. Geology 10:129–133

Miller CF, Mittlefehldt, DW (1984) Extreme fractionation in felsic magma chambers: a product of liquid-state diffusion or fractional crystallization? Earth Planet Sci Lett 68:151–158

Miller CF, Watson EB, Harrison TM (1988) Perspectives on the source, segregation and transport of granitoid magmas. Trans Royal Soc Edinburgh, Earth Sci 79:135–156

Mineyev DA (1963) Geochemical differentiation of the rare earths. Geokhimiya 12:1082–1100

Mittlefehldt DW, Miller CF (1983) Geochemistry of the Sweetwater Wash Pluton, California: implications for anomalous trace element behaviour during differentiation of felsic magmas. Geochim Cosmochim Acta 47:109–124

Neumann E-R (1980) Petrogenesis of the Oslo Region larvikites and associated rocks. J Petrol 21:498–531

Neumann E-R, Larsen BT, Sunvoll B (1985) Compositional variations among gabbroic intrusions within the Oslo Rift. Lithos 18:35–59

Neumann E-R, Brunfelt AO, Finstad, KG (1977) Rare earth elements in some igneous rocks in the Oslo Rift, Norway. Lithos 10:311–319

Neumann E-R, Pallesen S, Andresen P (1986) Mass estimates of cumulates and residues after anatexis in the Oslo graben. J. Geophys Res 91:11629–11640

Neumann E-R, Tilton GR, Tuen E (1988a) Sr, Nd and Pb isotope geochemistry of the Oslo Rift igneous province, southeast Norway. Geochim Cosmochim Acta 52:1997–2007

Neumann E-R, Andersen T, Mearns EW (1988b) Olivine clinopyroxenite xenoliths in the Oslo Rift, SE Norway. Contrib Mineral Petrol 98:184–193

Neumann E-R, Sundvoll B, Øverli PE (1990) A mildly depleted upper mantle beneath southeast Norway: evidence from basalts in the Permo-Carboniferous Oslo Rift. Teconophysics 178:89–107

Olsen KI, Griffin WL (1984a) Fluid inclusion studies of the Drammen Granite, Oslo Paleorift, Norway. I. Microthermometry. Contrib Mineral Petrol 87:1–14

Olsen KI, Griffin WL (1984b) Fluid inclusion studies of the Drammen Granite, Olso Paleorift, Norway. II. Gas- and leachate analyses of miarolytic quartz. Contrib Mineral Petrol 87:15–23

Olsen KH, Baldridge WS, Larsen BT, Neumann E-R, Ramberg IB (1987) A lithospheric transect across the Oslo Paleorift, Norway. Eos Trans Am Geophys Union 68:1480

Parrish RR (1990) U-Pb dating of monazite and its application to geological problems. Can J Earth Sci 27:1431–1450

Pearce JA, Harris NBW, Tindle AG (1984) Trace element discrimination diagrams for the tectonic interpretation of granitic rocks. J Petrol 25:956–983

Pedersen S, Maaløe S (1990) The Iddefjord granite: geology and age. Norges Geol Unders Bull 417:55–64

Presnall DC, Dixon SA, Dixon JR, O'Donnell TH, Brenner NL,

Schrock RL, Dycus DW (1987) Liquidus phase relations on the join diopside-forsterite-anorthite from 1 atm to 20 kbar: their bearing on the generation and crystallization of basaltic magma. Contrib Mineral Petrol 66:203–220

Presnall DC, Dixon Jr, O'Donnell TH, Dixon SA (1979) Generation of mid-ocean ridge tholeiites. J Petrol 20:3–35

Ramberg IB (1976) Gravity interpretation of the Oslo Graben and associated igneous rocks. Norges Geol Unders 325:184 pp

Ramberg IB, Larsen BT (1978) Tectonomagmatic evolution. In: Dons JA, Larsen BT (ed) The Oslo Paleorift. A review and guide to excursions. Norges Geol Unders 337:55–73

Rasmussen E, Neumann E-R, Andersen T, Sundvoll B, Fjerdingstad V, Stabel, A (1988) Petrogenetic processes associated with intermediate and silicic magmatism in the Oslo Rift, south-east Norway. Min Mag 52:293–307

Segalstad TV (1979) Petrology of the Skien basaltic rocks. Lithos 12:221–239

Shand SJ (1949) Eruptive rocks. Wiley, New York

Sigmond EMO, Gustavsen M, Roberts D (1984) Bedrock map of Norway, 1:1 million. Geol Surv Norway

Stenstrop G (1989) Anorogenic complexes associated with molybdenum mineralizations. Part I. Petrogenesis of the Finnemarka zoned complex and associated molybdenum mineralization. Thesis, Aarhus University, Aarhus, Denmark

Sundvoll B (1978) Isotope and trace element geochemistry. In: Dons JA, Larsen BT (eds) The Oslo Paleorift. A review and guide to excursions. Norges Geol Unders 337:35–40

Sundvoll. B, Neumann E-R, Larsen BT, Tuen E (1990) Age relations among Oslo Rift magmatic rocks: implications for tectonic and magmatic modelling. Tectonophysics 178:67–87

Taylor HP, Strong DF, Fryer BJ (1981) Volatile control of contrasting trace element distribution in peralkaline granitic and volcanic rocks. Contrib Mineral Petrol 77:267–271

Turpin L, Cuney M, Friedrich M, Bouchez JL, Aubertin A (1990) Meta-igneous origin of Hercynian peraluminous granites in N.W. French Massif Central: implications for crustal history reconstructions. Contrib Mineral Petrol 104:163–172

Wessel P, Husebye ES (1987) The Oslo Graben gravity high and taphrogenesis. Tectonophysics 142:15–26

Whalen JB, Currie KL, Chappell BW (1987) A-type granites: geochemical characteristics, discrimination and petrogenesis. Contrib Mineral Petrol 95:407–419

White AJR, Chappel BW (1988) Some supracrustal (S-type) granites of the Lachlan Fold Belt. Trans Royal Soc Edinburgh, Earth Sci 79:169–182

Wilson MR (1982) Magma types and tectonic evolution of the Swedish Proterozoic. Geol Rundsch 71:120–129

Zen E-A (1986) Aluminum enrichment in silicate melts by fractional crystallization: some mineralogic and petrographic constraints. J Petrol 27:1095–1117

Zindler A, Hart S (1986) Chemical geodynamics. Ann Rev Earth Planet Sci 14:493–571

Editorial responsibility: J. Patchett